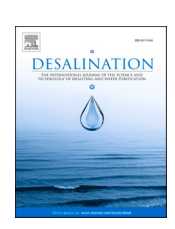
ELSEVIER

## Contents lists available at ScienceDirect

# Desalination

journal homepage: www.elsevier.com/locate/desal





# Designs and performance analysis of vertical multi-effect diffusion solar distiller: A review

Byung-Ju Lim, Ph.D. <sup>a</sup>, Seok-Min Choi, Ph.D. <sup>a</sup>, Sung-Hoon Cho, Ph.D. <sup>a</sup>, Ga-Ram Lee, Master <sup>a,b</sup>, Chang-Dae Park, Ph.D. <sup>a,b,\*</sup>

- <sup>a</sup> Department of Plant Technology Energy Systems Research Division, Korea Institute of Machinery & Materials, 156 Gajeongbuk-ro, Yuseong-gu, Daejeon 34103, Republic of Korea
- <sup>b</sup> Department of Plant system and Machinery, University of Science & Technology, 217 Gajeong-ro, Yuseong-gu, Daejeon 34113, Republic of Korea

#### HIGHLIGHTS

- This paper reviews a vertical multiple effect solar distiller (VMED) studied since 1964.
- VMEDs with basin, curved plate, and tilted wick still have been in the spotlight recently.
- VMEDs with basin and reflector have the most productivity.
- More studies are needed to secure reliability for the long-term operation.
- Experimental studies on classical VMED in various solar conditions are needed.

#### ARTICLE INFO

#### Keywords: Solar desalination Multi-effect diffusion Solar still Design Performance

#### ABSTRACT

Owing to the rapid growth of the world's population and water contamination due to industrialization, water scarcity is becoming increasingly worse. Solar desalination is a promising technique to obtain freshwater without carbon generation. A vertical multiple-effect diffusion solar distiller (VMED), among solar desalination systems, has a simple structure and small size, and its production is higher than a conventional solar still. VMED comprises a series of closely spaced parallel plates and can efficiently get the freshwater by repeatedly using the input solar energy. Researchers have gradually tried to improve the performance of various VMEDs. This paper reviews the detailed design and performance of eight types of VMEDs; classic VMED, VMED with a solar collector, VMED with an external heat source, VMED with a reflector, VMED with a basin, VMED with a curved plate, VMED with a tilted wick still, and a horizontal VMED. Additionally, the performance effect and optimum values are analyzed according to critical parameters, including environmental, design, and operating parameters. This review determined the design characteristics of VMEDs, optimal variables and their effects on production, and the best VMED design. This review will help the researchers develop novel VMEDs with high performance.

# 1. Introduction

Freshwater demands have been increasing worldwide because of climate changes, industrialization, and population growth; however, most available water is salty or impure. Solar desalination is a promising technique to obtain freshwater without carbon generation. Although

other renewable energy resources such as wind power, geothermal energy, and bioenergy are available for water desalination, solar distillation has become more prevalent recently, particularly in rural areas [1]. Techniques of solar distillation have been employed and advanced over centuries. A typical solar desalination unit such as the conventional solar still (CSS) (or a single-slope basin-type solar still) (Fig. 1), which has a simple design, can be easily manufactured with locally available

Abbreviations: CSS, conventional solar still; MED, multiple effect diffusion solar distiller; PR, performance ratio; VMED, vertical multiple-effect diffusion solar distiller.

E-mail addresses: bzoo77@kimm.re.kr (B.-J. Lim), choism@kimm.re.kr (S.-M. Choi), shcho75@kimm.re.kr (S.-H. Cho), ccl3455@kimm.re.kr (G.-R. Lee), parkcdae@kimm.re.kr (C.-D. Park).

https://doi.org/10.1016/j.desal.2022.115572

Received 1 November 2021; Received in revised form 4 January 2022; Accepted 13 January 2022 Available online 20 January 2022

<sup>\*</sup> Corresponding author at: Department of Plant Technology Energy Systems Research Division, Korea Institute of Machinery & Materials, 156 Gajeongbuk-ro, Yuseong-gu, Daejeon 34103, Republic of Korea.

Nomer	ıclature	d	day
		dr	direct
$c_p$	specific heat capacity	df	diffuse
ď	distance or diffusion gap, mm	e	evaporation
D	diffusion coefficient of water vapor	es	evaporation surface
G	solar irradiance	f	feed water
h	enthalpy	g	cover glass
m	water production, kg/(m <sup>2</sup> ·d) or water production rate, kg/	glb	global
	$(m^2 \cdot h)$	in	inlet
ṁ	mass flow rate, kg/s or g/min	L	latent heat
N	the number of effects	out	outlet
p	saturated pressure or pressure, Pa	p	plate
Q	solar irradiance or heat transfer energy	r	radiative heat transfer
R	gas constant of water vapor	slr	solar radiation
T	temperature, °C	t	total
		w	seawater on condensation surface
Subscri			
ab	absorber	Greek	
amb	ambient	α	absorptance
av.	average	β	solar altitude angle
c	convective heat transfer	$\theta$	inclination angle to ground
cd	conductive heat transfer	τ	transmittance
cs	condensation surface	ξ	azimuth angle

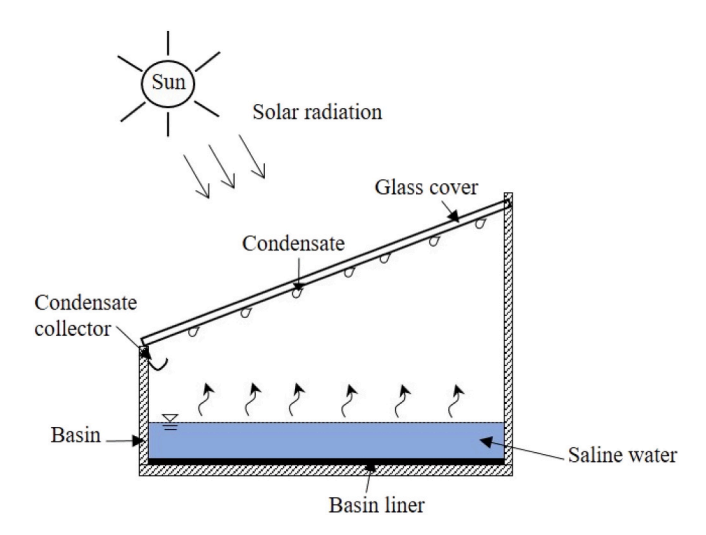


Fig. 1. Conventional basin-type solar still.

material and requires low maintenance [2]. However, a major drawback of the CSS is the low freshwater yield, which depends on the season, region, and intensity of solar radiation [3]. Therefore, many researchers have attempted to develop new designs and technologies for enhancing the CSS performance by adopting the following measures: 1) installing fins in a basin to increase heat transfer from a basin to water [4,5], 2) using a stepped basin to increase the evaporation rate from a basin [6-8], 3) applying heat storage materials in a basin to increase the evaporative and convective heat transfer coefficients [9,10], 4) applying double-slope cover glass to increase the intensity of solar irradiation [11–13], and 5) applying a multi-stage basin to reuse the latent heat of the condensate [14–16]. However, the production of freshwater using the advanced CSS is still insufficient (<10 kg/( $m^2$ -d)); therefore, the research on a solar distiller with better performance is in progress.

In 1959, a vertical multiple-effect diffusion solar distiller (VMED) was proposed [17] by Mária Telkes, who was a Hungarian–American biophysicist, scientist, and inventor working on solar energy

technologies. Subsequently, research on VMEDs has been going on and increased sharply since 2010, as shown in Fig. 2. Generally, a CSS obtains freshwater via a process of seawater evaporation in a basin and condensation onto a glass cover. In VMED, this process is repeated such that the heat of condensation is reused to drive the next evaporation process [18]. Using multiple effects can not only improve the performance and efficiency of the distiller but also reduce water cost. Therefore, studies on improving the performance by presenting new designs or adding other devices as well as optimizing the classical VMED have been consistently conducted. Existing studies have revealed the effects of various parameters on the performance of VMED and their optimal values. However, there are cases where each variable's optimal values or trends do not agree with each other; therefore, it is necessary to organize and analyze them more systematically.

Although several studies have been conducted on VMEDs since 1959, to the best of our knowledge, no comparative analysis of these studies has been conducted thus far. To conduct future research on VMEDs more

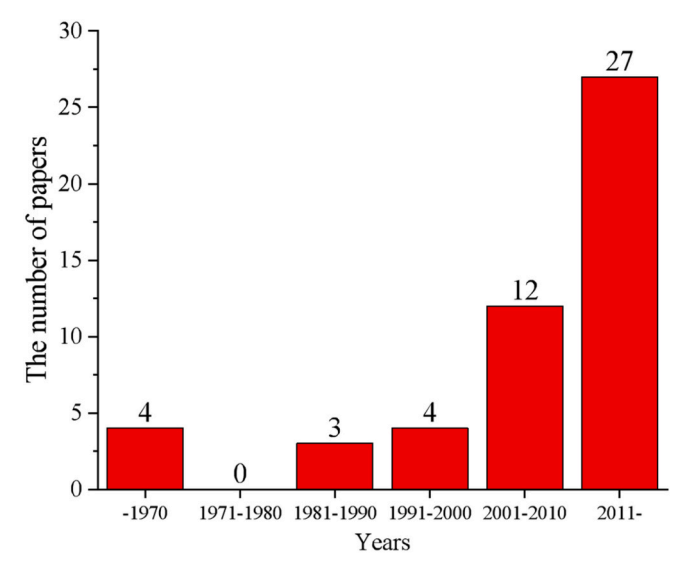


Fig. 2. Number of research papers on the VMEDs in different years.

efficiently, comprehensive, well-organized information is required about developed VMEDs.

In this review, we present a comprehensive evaluation of different VMED designs developed thus far by several researchers. Additionally, we evaluated the performance of VMEDs across different types and conditions as well as analyzed the influence of various parameters on the performance and their optimum values. Finally, future research activities aimed at improving and commercializing VMEDs are presented.

## 2. Working principle and components of VMED

Fig. 3 illustrates the schematic of VMED. VMED comprises several closely spaced parallel plates. The first plate in the distiller is colored black and absorbs solar radiation. A transparent cover glass on front of the first plate is installed with an air gap to reduce heat loss from the absorber plate. Feed saline water is supplied to the evaporation surface of all effect plates above the distiller. The temperature of the feed saline water on the evaporation surface increases due to the thermal energy transferred from the first plate; consequently, the saline water is evaporated. The evaporated water vapors diffuse and condense on the front surface of the next effect plate, and then the discharged latent heat of condensation is transferred to the saline water flowing down the plate's rear surface. Such evaporation and condensation processes repeatedly occur from the first to the last effects of the VMED. A fabric wick is usually attached to the evaporation surface to evenly spread the feed saline water over the vertical plate and allow the water to slowly flow down. Instead of the wick, troughs can be used to trap the feed water. The vapor from the evaporation surface forms condensate droplets that flow down because of their weight when they continue to grow. A ditch is installed at the bottom of the condensing surface to collect the distillate. VMED is slantly installed to increase the absorption of solar radiation. It is known that the absorption rate increases as the installation inclination angle  $(\theta)$  of a solar collector is similar to the latitude installed [19].

#### 3. Numerical modeling of VMED

The heat and mass transfer in a solar still is considered as the transient process due to the variation in the temperature or heat flux with respect to time [20]. This review introduces the heat and mass transfer models of the VMED to completely understand the phenomena in the still.

# 3.1. Cover glass and solar absorber

The energy balance for the cover glass can be expressed as follows:

$$(mc_p)_g \frac{dT_g}{dt} = Q_{slr,g} + Q_{r,ab} + Q_{c,ab} - Q_{c,amb} - Q_{r,amb}$$
(1)

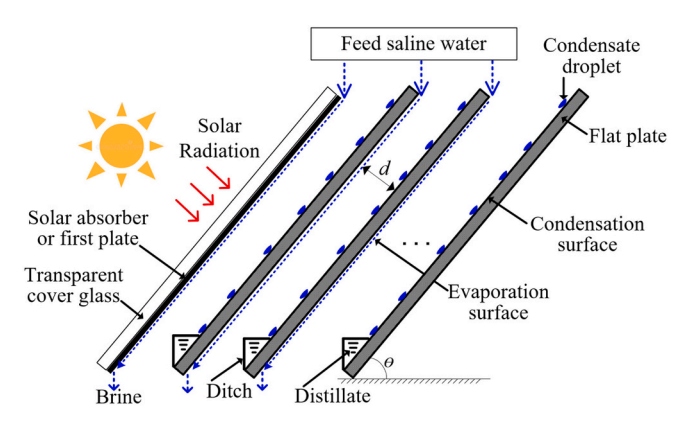


Fig. 3. Schematic of the classical VMED.

$$Q_{slr,g} = \alpha_g G_{dr} \left( cos\theta + sin\theta \frac{cos\xi}{tan\alpha} \right) + \alpha_g G_{df} \left( \frac{1 + cos\theta}{2} \right)$$
 (2)

In Eq. (1),  $Q_{slr,g}$  is the energy absorbed by the cover glass from solar radiation,  $Q_{r,ab}$  and  $Q_{c,ab}$  are the radiative and convective heat transfer energy from the solar absorber (or first plate) to the cover glass, respectively, and  $Q_{c,amb}$  and  $Q_{r,amb}$  are the energy released from the cover glass to the surrounding by convection and radiation, respectively.  $c_p$  is specific heat capacity at constant pressure. In Eq. (2),  $G_{dr}$  and  $G_{df}$  are direct and diffusion solar irradiance, respectively and  $\alpha_g$  is absorptance of the cover glass.

The energy balance for the solar absorber can be expressed as follows:

$$(mc_p)_{ab} \frac{dT_{ab}}{dt} = Q_{slr,ab} - Q_{r,ab} - Q_{c,ab}$$
(3)

$$Q_{slr,ab} = \tau_g \alpha_{ab} G_{dr} \left( cos\theta + sin\theta \frac{cos\xi}{tan\beta} \right) + \tau_g \alpha_{ab} G_{df} \left( \frac{1 + cos\theta}{2} \right)$$
 (4)

where  $Q_{slr,ab}$  is the solar radiation energy absorbed by the solar absorber,  $\tau_g$  is the transmittance of the cover glass, and  $\alpha_{ab}$  is the absorptance of the solar absorber.

## 3.2. Evaporator and condenser

The energy equation for the evaporating surface of the effect plates is shown in Eq. (5).

$$\left(mc_{p}\right)_{w}\frac{dT_{w}}{dt}=Q_{in,ev}-\left(Q_{r}+Q_{c}+Q_{L}\right)_{ev}+h_{f}\left(\dot{m}_{f,in}-\dot{m}_{f,out}\right)$$
(5)

where  $Q_r$  and  $Q_c$  are radiative and convective heat transfer to the next effect plate, respectively.  $Q_L$  is the latent heat of evaporation for feed water in the evaporation surface.  $Q_{in,ev}$  is the energy supplied to evaporation surface. In the first effect,  $Q_{in,ev}$  is same with  $Q_{slr,ab}$  of Eq. (4), but in other effects, the value of that is the summation of  $Q_r$ ,  $Q_c$ , and  $Q_L$ .  $h_f$  is enthalpy of feed water.  $m_{f,in}$  and  $m_{f,out}$  are mass flow rate of the feed water and the brine, respectively. The amount of vaporized seawater  $(m_e)$  is to subtract  $m_{f,out}$  from  $m_{f,in}$  and can be calculated by Eq. (6).

$$\dot{m}_e = \frac{Dp_t}{RT_{av}d} \times ln \left(\frac{p_t - p_{cs}}{p_t - p_{es}}\right) \tag{6}$$

where D is the diffusion coefficient of water vapor, and  $T_{av}$  is the average evaporation and condensation surface temperature of the next effect plate. The value of gas constant of water vapor (R) was 461.6 J/(kg•K). d is the diffusion gap between effect plates.  $p_t$  is total pressure,  $p_{cs}$  is the saturated water vapor pressure of the condensation surface of the next effect plate, and  $p_{es}$  is the saturated seawater vapor pressure of the evaporation surface.

The energy equation of the condensation surface is shown in Eq. (7).

$$(mc_p)_p \frac{dT_p}{dt} = Q_{in,p} - Q_{cd,p} \tag{7}$$

where  $Q_{in,p}$  is the energy transferred from the evaporation surface to the condensation surface and is the summation of the values of  $Q_r$ ,  $Q_c$ , and  $Q_L$  in Eq. (5).  $Q_{cd,p}$  is conductive heat transfer energy within the effect plate.

### 3.3. Assumptions

The followings are the primary assumptions used in the numerical modeling [21-23]:

- The thermal losses through the sides are negligible.
- The temperature of the cover glass and each plate is uniform.

- Thermal losses by conduction are negligible.
- The water film on the evaporator is very thin.
- The temperature drop within the plates is negligible.
- The inlet temperature of the feed water is the same as the ambient
- The evaporated water vapor on evaporation surface moves only horizontally, and condenses fully on the next flat plate.

### 4. Performance index of a distiller

The performance of a distiller is expressed in terms of daily production and performance ratio (PR). For the daily output, the total amount of freshwater produced with respect to the unit installation area or solar collecting area is often used for comparison between devices as shown in Eq. (8).

$$m_d = \frac{Daily\ total\ amount\ of\ water}{installation\ area\ or\ solar\ collecting\ area} \tag{8}$$

For VMED, the production based on the installation area is relatively very high because the unit is vertically installed. Therefore, it is rational to express the production based on the solar collecting area, i.e., the area of the first plate (Fig. 3). In this paper,  $m_d$  is calculated on the basis of the solar collecting area. PR is generally a measure of how effectively heat energy is reused for freshwater production [24] and is defined as a ratio of latent heat of produced freshwater to the energy input. PR is calculated as follows:

$$PR = \frac{m_d \times h}{\sum Q_{in}} \tag{9}$$

where  $Q_{in}$ , the input energy to solar still, denotes the amount of incident radiation on the heat-collecting surface when operating under sunlight; however, when using external heat sources it denotes the energy transferred to the still.

In 1973, Cooper [25] claimed that the maximum PR of CSS was 0.6 through theoretical research and it would be difficult to obtain a value greater than 0.5 in practical installations.

## 5. Classification of VMEDs

# 5.1. Classical VMED

In 1964, Kudret Selçuk [21] developed a 2-effect VMED with double cover glass (Fig. 4). On one side of the plate, this VMED featured several troughs that served as the evaporation surfaces. When the feed water was supplied to the top troughs, the water level gradually increased to the height of the tubes installed in the troughs, and the seawater overflowed from the tubes to feed the troughs placed below. Because the troughs were placed vertically in series, the seawater supplied by the top

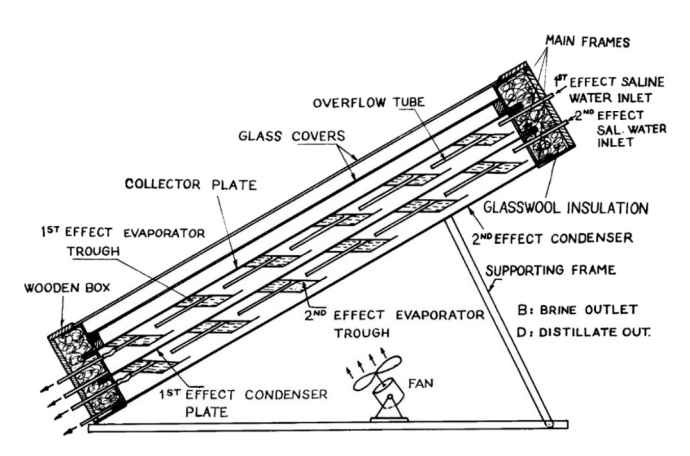


Fig. 4. Schematic of 2-effect VMED with troughs [21].

trough filled all the troughs placed below. The results indicated that the VMED outperformed a conventional roof-type still. However, Kudret Selçuk was concerned about the relatively high initial cost, and plastic materials were proposed to reduce the cost of production when practical uses were considered.

In 1987, Ouahes et al. [26] investigated the performance of the 3-effect VMED (Fig. 5). They constructed and performed experiments with two types of VMED. First, a 3-effect VMED prototype was developed with plate sizes of  $20 \times 25$  cm² and d=10 mm. The small VMED prototype was operated in the laboratory under Xenon lamp irradiation and was then operated over two summer seasons under Algiers sunshine. Then, a 3-effect VMED of  $1 \times 0.5$ -m² size and d=40 mm was used for the experiment under artificial radiation using a heating lamp. The experimental results showed that VMED produced a distillate of 1.092 kg/(m²-h) at input energy of  $408 \text{ W/m}^2$ .

In 1996, Ohsiro et al. [27] proposed a VMED comprising an evaporating wick, a condensing wick, and a hydrophobic poly(tetrafluoroethylene) (PTFE) net (Fig. 6). A 2.0-mm PTFE net was sandwiched between a 0.65-mm thick cotton wick with an evaporation area of  $0.3 \times 0.42 \text{ m}^2$  and the condensing wick (Fig. 7). The condensing wick was a 0.45-mm thick polyester cloth glued onto a 5-mm thick aluminum plate, the bottom surface of which was in contact with a plastic cooling jacket. The PTFE net reduced d considerably. Water vapor diffused from the evaporating wick to the condensing wick through the net's gaps. Because of its low wettability, the net could prevent saline water from contaminating of the condensate. Theoretical results showed that the  $m_d$  of a 10-effect VMED with a PTFE net was  $4.932 \, \text{kg/(m}^2 \cdot \text{h})$  at a constant power of  $1 \, \text{kW/m}^2$ .

In 1998, Bouchekima et al. [28] performed experiments using a VMED (Fig. 8) installed in Touggourt, the south of Algeria where groundwater temperature was  $\sim$ 65 °C. The effect plates with an area of 1  $\times$  0.5 m² were made of aluminum and placed 40-mm apart. They recommended using a porous gauze as a wick material to form a capillary film. Experimental results showed that the efficiency of the VMED increased with the temperature of the inlet feed water and the solar irradiation. In solar conditions, their single-effect VMED produced freshwater of 0.56 kg/(m²-h) at  $T_f = 45$  °C. Additionally, the 2-effect VMED obtained 0.84 kg/(m²-h) at  $T_f = 42.5$  °C, and the production

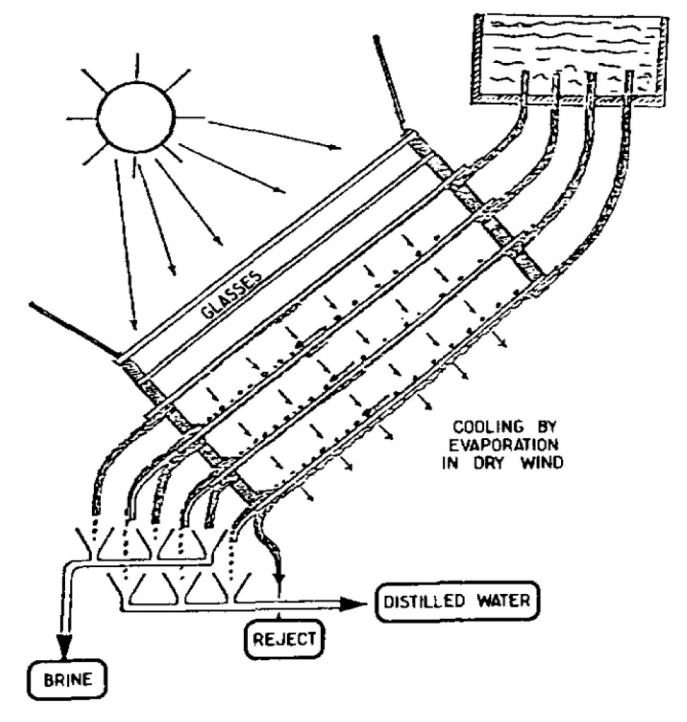


Fig. 5. Schematic of 3-effect VMED [26].

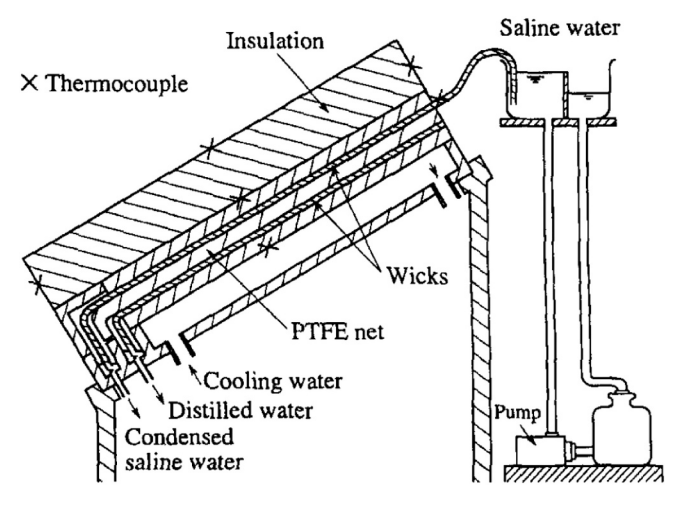


Fig. 6. Schematic of VMED with a PTFE net [27].

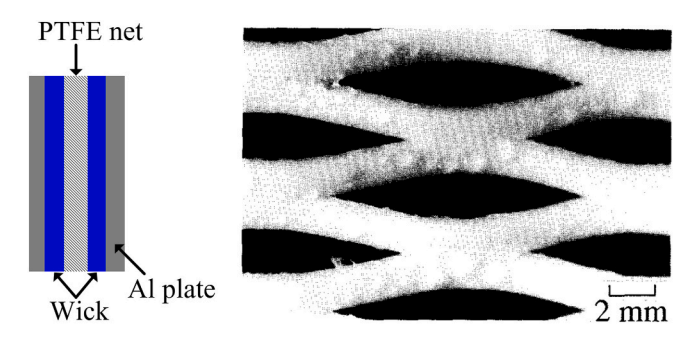


Fig. 7. Effect's configuration using a PTFE net [27].

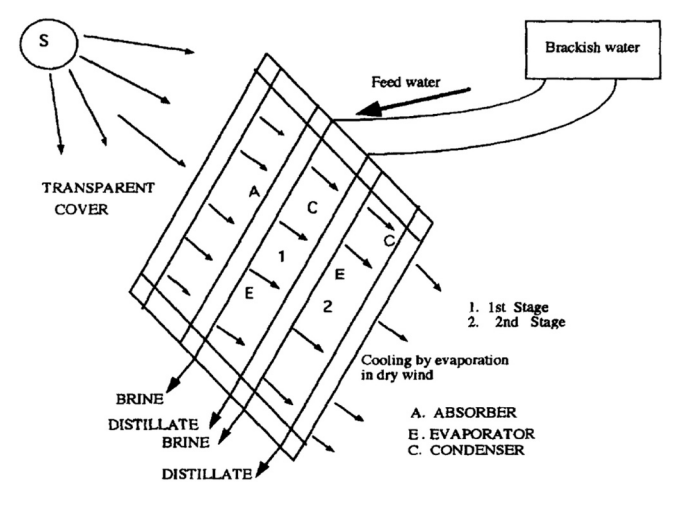


Fig. 8. Schematic of the VMED presented by Bouchekima et al. [28].

was 1.5 times higher than that of a single-effect VMED.

In 2018, Lim et al. [29,30] performed parametric studies on VMEDs with a single and a double glass cover (Fig. 9). They developed a two-dimensional (2D) numerical model of the VMED to analyze the design and operation parameters, such as  $\dot{m}_f$ ,  $\theta$ , wind speed, and  $N_t$ . For the VMED with single glass cover [29], the results showed that the  $m_d$  was 16.6 kg/(m²·d) by optimal operation, and PR was 1.44, which was 2.8 times higher than that of the CSS. However, the wind decreased the yield of the distiller due to heat loss from the glass. Although the productivity increased with decreasing  $\theta$ , the optimum value of  $\theta$  was in the range of  $40^\circ$ – $50^\circ$ , considering the deformation of the plate by its weight and the

contamination of freshwater. The recommended  $m_f$  was 6 g/min for all effects on basis of the effect size of 1 m², and the optimal  $N_t$  was 11 based on both the annual productivity and manufacturing cost of the VMED. In 2020, for VMED with a double glass cover [30], they focused on determining the maximum productivity and lowering the water cost by optimizing various parameters. The results showed that the optimum values of the gap distance of the double glass cover and  $N_t$  were in the ranges of 25–30 mm and 10–15, respectively. Additionally, the  $m_f$  during spring, summer, fall, and winter was optimal at 9, 16, 10, and 3 g/min, respectively. The maximum productions for all seasons (spring, summer, fall, and winter) were 16.6, 36.0, 19.0, and 2.5 kg/(m²-d), respectively, in South Korea. The economic analysis showed that the water cost was 6.1 \$/m³, which was more competitive in the market of a small capacity of <100 m³/d.

In 2020, Lee et al. [31] focused on developing VMED with an integrated effect plate without a wick. They stated that attaching a wick to the plate increases the manufacturing time and cost, and the detachment of an old wick from the plate causes a decrease in the still's performance and reliability. They selected seven characteristics required for a wickfree plate (WFP) and fabricated the WFP specimens such as an etching plate, a three-dimensional (3D)-printing plate, and a porous metal plate (Fig. 10). Experimental results showed that the grooved etching plate was appropriate for a WFP, and the optimum patterned shapes and their sizes were pitch = 3.5 mm, furrow = 3.0 mm, and depth = 2.0 mm. The outdoor experiment showed that 3-effect VMEDs with the WFP produced 4.4% more freshwater (3.55 kg/( $m^2$ ·d)) than those with a wick. In 2021, Lee et al. [32] showed that with varying the seawater feed flow rate, the production stability of the VMED using WFP was better than that of VMED with a wick. They insisted that this behavior of a WFPbased multiple-effect diffusion solar distiller (MED) is attractive when considering the practical difficulty in adjusting the optimum flow rate during real operations in the field.

In 2020, Xu et al. [33] developed a small-sized 10-effect VMED with a plate of  $0.01\text{-m}^2$  area and d=5 mm (Fig. 11). This device comprised 11 nylon frames (Nylon PA12) made via 3D printing. A monolithic 5-mm thick silica aerogel was placed between the solar absorber and glass cover as a transparent thermal insulation. The indoor experimental results showed that the distiller produced freshwater of  $5.78 \text{ kg/(m}^2\text{-h})$  at a uniform power of  $1 \text{ kW/m}^2$  supplied by the solar simulator. Furthermore, they performed an outdoor experiment at the MIT (Massachusetts Institute of Technology) campus (of USA) on a partly sunny day with scattered clouds. The production of VMED with  $\theta=60^\circ$  was 0.072 kg for 4.5 h ( $m_d=1.6 \text{ kg/(m}^2\text{-h})$ ).

In 2020, Sharon et al. [34] numerically studied the influence of various parameters on the performance and economics of VMED (Fig. 12). The results for performance parameters showed the following. 1)  $\dot{Q}_{slr}$  and  $T_{amb}$  positively affect the  $m_d$  and economics of the unit. 2) Wind over the glass cover reduced the productivity due to an increase in heat losses from the absorber plate. 3) An increase in  $N_t$  and a decrease in d enhanced the yield and PR. The most economical  $N_t$  value was 3. The annual average yield and exergy efficiency of VMED were approximately 11.13 kg/( $m^2$ ·d) and 13.75%, respectively.

#### 5.2. VMED with a solar collector

The classical VMED directly absorbs the solar radiation through the first plate, therefore it is generally installed in a slanting manner to improve performance. If the external solar collector absorbs solar energy and transfers it to the first plate, The VMED can be installed vertically. Lim et al. [30] stated that the classical VMED had limitations with respect to the inclination angle due to plate warpage and the contamination of distillate on the condensation surface. However, the installation angle of the solar collector can be decreased to receive the maximum solar energy. Besides, because only the area of the collector can be changed separately, the amount of solar energy is adjusted

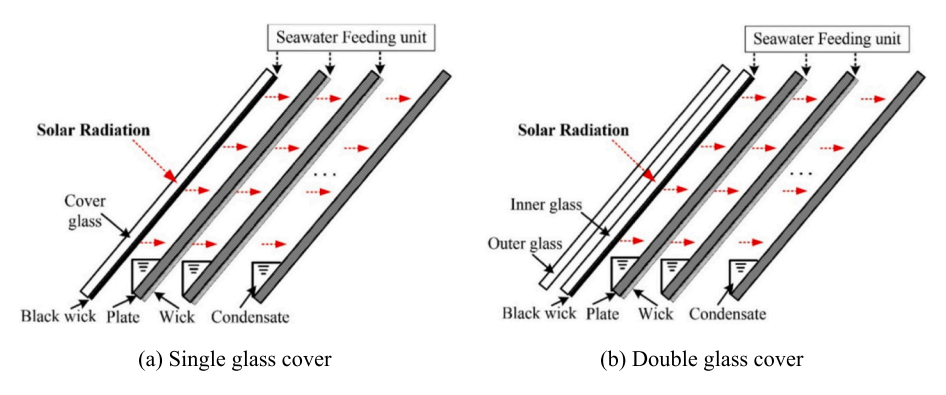


Fig. 9. Schematics of VMED designed by Lim et al. [30].

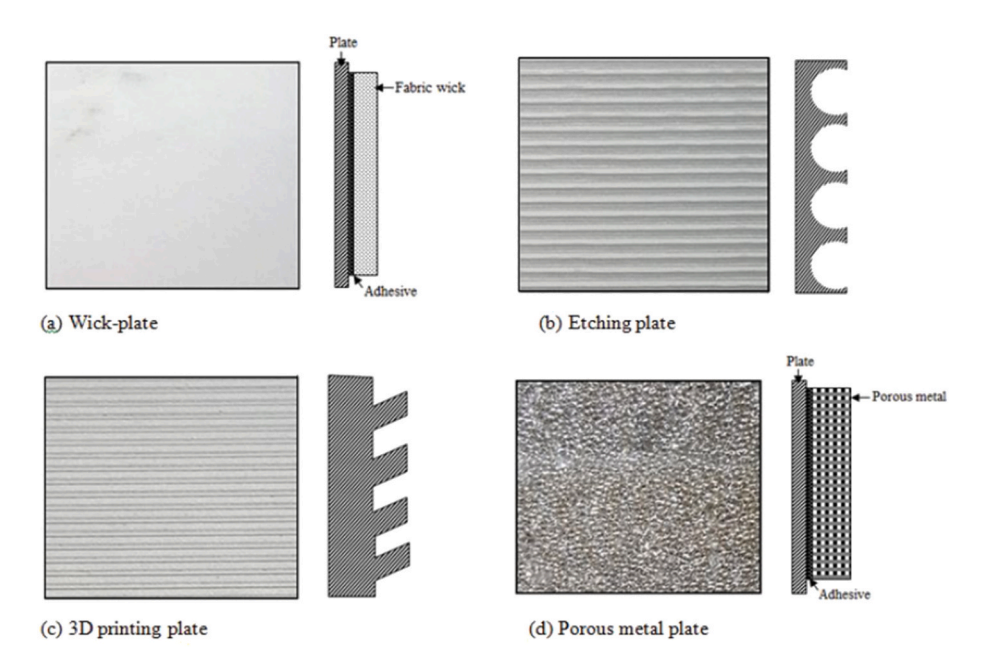


Fig. 10. Wick-plate and various WFPs for VMED [31].

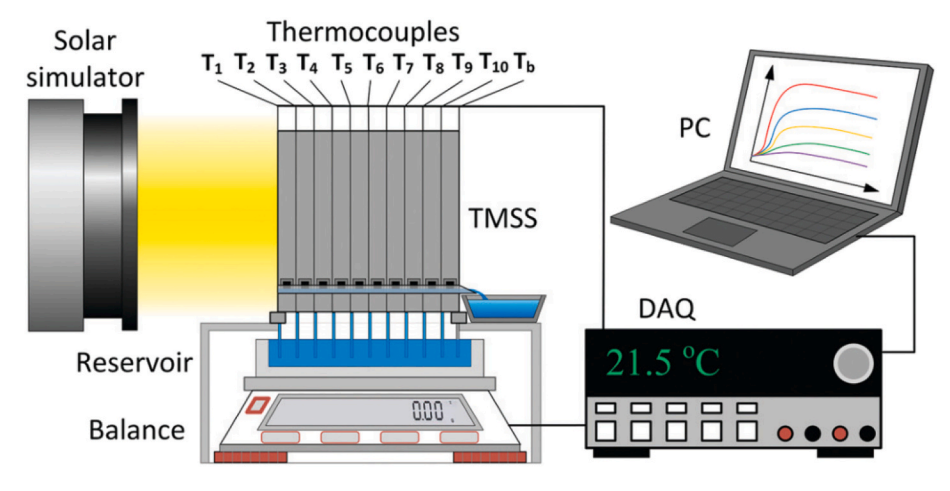


Fig. 11. Experimental setup for the mini VMED developed by Xu et al. [33].

without changing the plate size.

In 1961, Dunkle [35] focused on developing a theoretical model of VMED presented by Mária Telkes [17] in 1959 and experimentally validating the model. The author designed a small 5-effect VMED with a

solar absorber (Fig. 13) and operated it for seven months using an electric heater. The results showed that the distillation rate increased with a decrease in d, and using  $H_2$  gas as the diluent gas is better than using the air in the gap between plates. Besides, the ratio of feed rate to

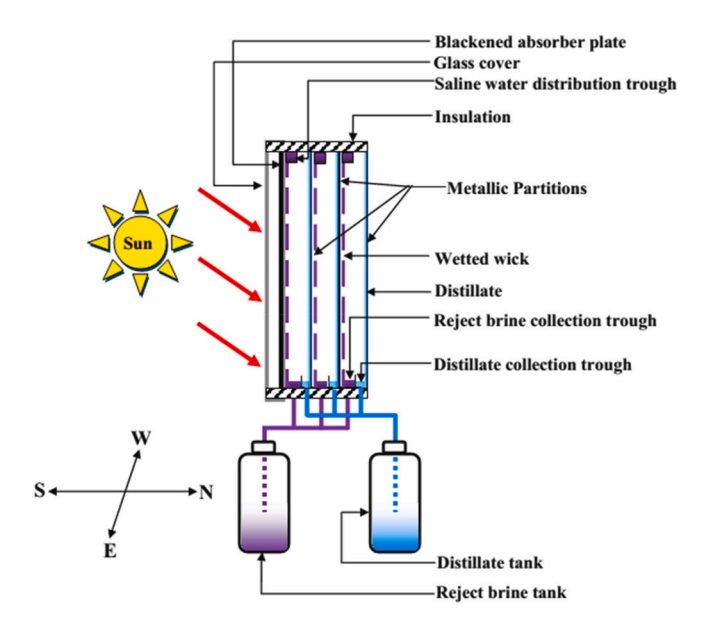


Fig. 12. Schematic of the 3-effect VMED presented by Sharon et al. [34].

distillation rate  $(\dot{m}_f/\dot{m}_e)$  decreased with temperature, resulting in reduced heat losses into the brine. However, the author warned about maintaining proper inlet feed water conditions and the problems of corrosion, sedimentation, scaling, and salt deposition.

In 1967, Cooper and Appleyard [36] developed a 3-effect VMED with solar absorber plates. The plates contacted the bottom surface effect still and used a saline-soaked wick. The still was inclined toward the sun. The radiation was transmitted through a glass cover that heated the first plate to cause evaporation from the plate.

In 1987, Kiatsiriroat et al. [37] presented an analytical model for predicting the performance of a 2-effect VMED using a flat-plate solar collector as a heat source (Fig. 14). The  $1.4\text{-m}^2$  flat-plate collector faced south and was inclined  $15^\circ$  from the horizontal direction. A pump transported the hot working fluid heated by the solar collector to the first plate of VMED. To prevent heat loss, the front side of the first plate  $(1.52\times0.9~\text{m}^2)$  was installed with a serpentine copper tube for heat exchange and insulated with a 50-mm thick Styrofoam. The main

parameters for numerical simulation were the solar radiation,  $T_{amb}$ , and wind speed. Numerical results showed that as the ratio of the evaporating surface area to the solar collector area increased, the distilled water output increased; however, when the ratio was greater than 5, the productivity leveled off. Using the last condensing plate with a wetted cloth showed better productivity than the bare plate cooled by ambient air. It was found that the distillation output increased with effect plate number but became stable when  $N_t$  was >5. Numerical results showed that the maximum output was  $6.0 \, \text{kg/(m}^2 \cdot \text{d})$  in April, but the experiment showed  $2.08 \, \text{kg/(m}^2 \cdot \text{d})$  under  $Q_{gls} = 13.0 \, \text{MJ/(m}^2 \cdot \text{d})$ .

During 2004-2005, Tanaka et al. [38-40] numerically and experimentally studied a VMED comprising a heat-pipe solar collector (Fig. 15). The solar collector was foldable or separable from VMED for easy transportation and low shipping costs. First, they focused on determining the effect of various parameters such as d and  $N_t$  on the performance [40]. The production was 1.14 times higher at d = 3 mm than at d = 5 mm. They presented a method to find optimum  $N_t$  under given conditions such as production, manufacturing cost, and lifetime. The optimum  $N_t$  for d=3 and 5 mm was 9 and 11, respectively. The performance of the still was 21.8 kg/(m<sup>2</sup>·d) on a sunny autumn equinox day with  $Q_{ols} = 22.4 \text{ MJ/(m}^2 \cdot \text{d})$  and 13% greater than that of a VMED with a basin. An enlarged parametric study [39] was conducted for determining the effect of the design parameters such as d, the ratio of the solar collector area to each partition area, the solar collector's angle, and  $N_t$ , as well as the operating parameters, such as  $\dot{m}_f$  and  $T_f$ , on production. Productivity increased with  $N_t$  and the temperature of the saline water fed to the wicks. Productivity also increased with a decrease in d,  $\dot{m}_f$ , and the ratio of the solar collector area to each partition area. Notably, the solar collector's optimum angle was equal to the solar altitude angle. The increase in the rate of the yield was considerable when d was <7 mm. The productivity increased with an increase in  $T_{f_1}$  so they suggested using the long black tube in the feeding line to the wicks.

Following previous numerical studies, Tanaka et al. [38] experimented with the VMED comprising a solar collector using heating lamps instead of actual solar radiation as the heat source. They found that the experimental model agreed well with the numerical prediction, and the production rate was  $\sim\!93\%$  of what was predicted. The maximum production in a 4-effect VMED was  $\sim\!0.35\,\text{g/(m}^2\cdot\text{s)}$  at a glass cover radiation of 748 W/m².

In 2014, Huang et al. [41] studied VMED with a solar vacuum-tube collector (Fig. 16). They used a solar collector with six collection

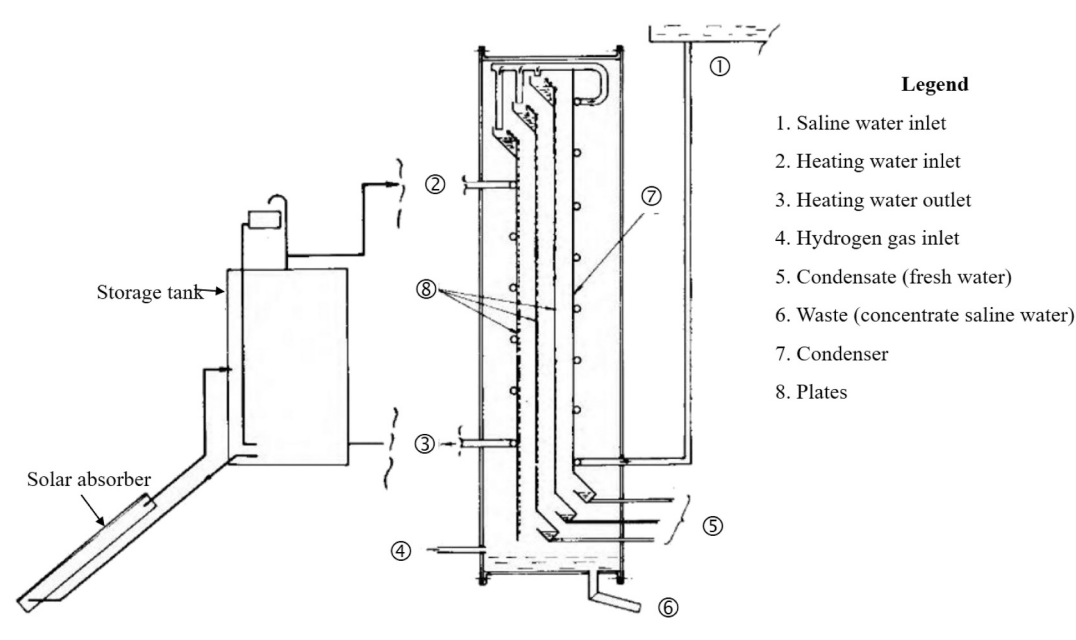


Fig. 13. Schematic of VMED made by Dunkle [35].

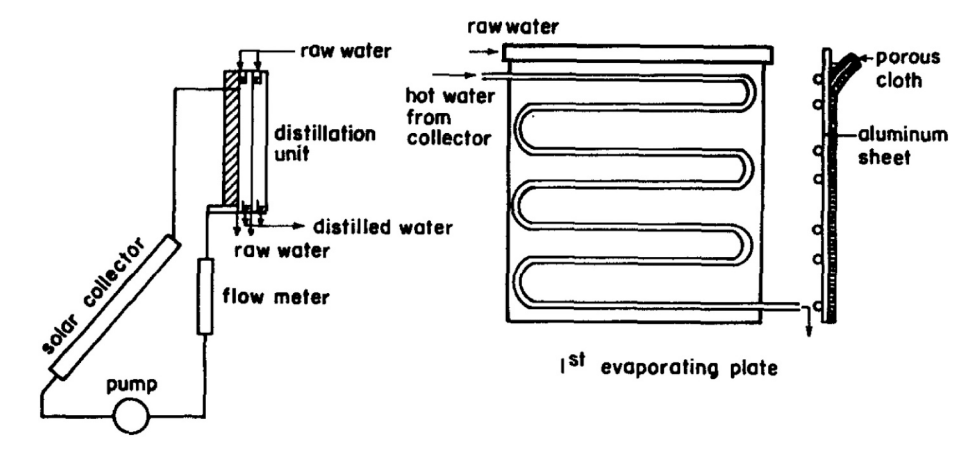


Fig. 14. Schematics of the 2-effect VMED with a solar collector [37].

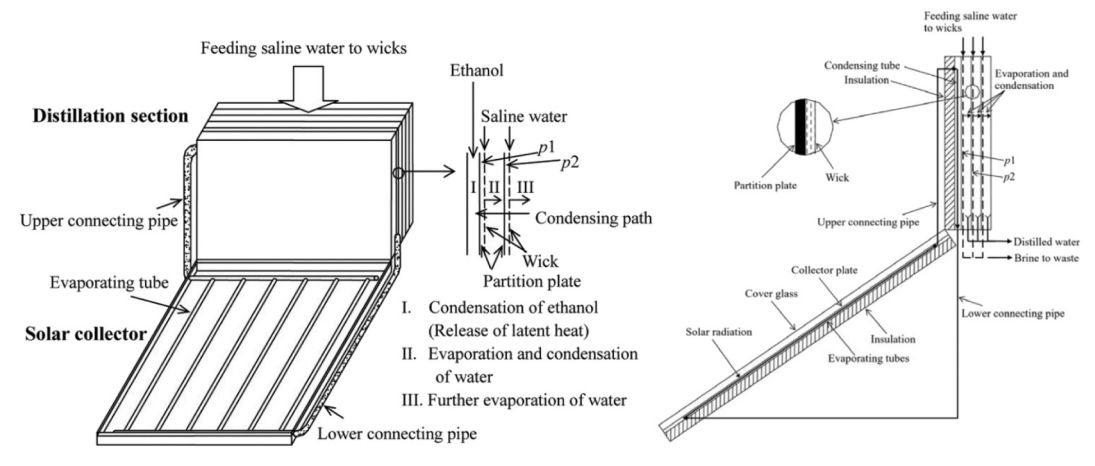


Fig. 15. Schematic of VMED designed by Tanaka et al. [40].

tubes and a total absorption area of 0.92 m². The VMED had a d of 6 mm. The solar heat absorbed by the solar collector evaporated the medium water and produced high-temperature steam as the heat source. The numerical results indicated that a 10-effect VMED produced about 13.7 and 19.7 kg/(m²·d) in 600 and 800 W/m², respectively. For a 20-effect

MED, the  $m_d$  (for 6 h) was  $\sim 16.5$  kg/d (17.9 kg/(m<sup>2</sup>·d)) and 23.7 kg/d (25.8 kg/(m<sup>2</sup>·d)) in Taiwan and a desert area, respectively. The yield rate of the 20-effect VMED increased by 32% compared with that of the 10-effect VMED.

In 2016, Reddy and Sharon [42] numerically studied the yield



Fig. 16. VMED with solar vacuum collector [41].

performance of VMED with a solar collector and a vacuum pump (Fig. 17). The VMED system comprised an upper solar collector, a saline water storage tank, and a VMED unit. The saline feed water tank was positioned at the left side of the last plate and acted as the condenser for the last effect. The feed saline water was transferred from the tank to the solar collector at the top of the system using a pump. The feed water was heated by solar energy and supplied to each effect plate. The vacuum pump was used to reduce the pressure in each effect unit. Various parameters such as  $N_t$ ,  $\dot{m}_f$ , d, the salinity of feed water, climate conditions, and operating pressure of the distillation unit were studied for determining their effect on the distillate yield. The maximum annual average of the yield was 21.29 kg/(m<sup>2</sup>·d) under a low-pressure condition of 0.25 bar; however, the average of 6.78 kg/(m<sup>2</sup>·d) was obtained under normal pressure. The average PR of VMED operating under evacuation mode was approximately 5.59, 4.44, and 3.52 for 0, 5, and 10 wt% of saline feed water, respectively. The yield increased by  $\sim$ 7% when d was reduced 40 to 5 cm. They found that the optimum  $N_t$  was 5, and in real conditions, a small  $\dot{m}_f$  value caused problems such as the choking of the feed water distributor with salt deposition, hence the optimum  $\dot{m}_f$  was 24 g/min.

In 2020, Ghadamgahi et al. [43] developed a 5-effect VMED with a solar collector, which had a paraffin wax storage unit with paraffin as phase change material (PCM) (Fig. 18). The VMED had aluminum effect plates with a thickness of 1 mm, a size of  $0.5 \times 0.5$  m<sup>2</sup>, and a plate separation of 10 cm. The outdoor tests were performed in Tehran's weather conditions from 08:00 to 20:00 during July and August 2018. The main parameters for the experiment were the thickness of the PCM and  $\dot{m}_f$ . The results showed that VMED with a 2.5-cm thick PCM increased the freshwater production by 15% compared with VMED without PCM, and the highest yield of water was 4.9 kg/(m<sup>2</sup>·d) for  $\dot{m}_f = 5.2$  g/(m<sup>2</sup>·min).

The design of VMED with solar collector has altered since the beginning of the project, from a separate unit to the one that is integrated into the VMED as a single device. Accordingly, simplification and performance optimization were considered for the practical application of the solar distiller.

## 5.3. VMED with an external heat source

For receiving thermal energy from external devices, VMED has the advantage of being able to use various heat sources. The preceding solar

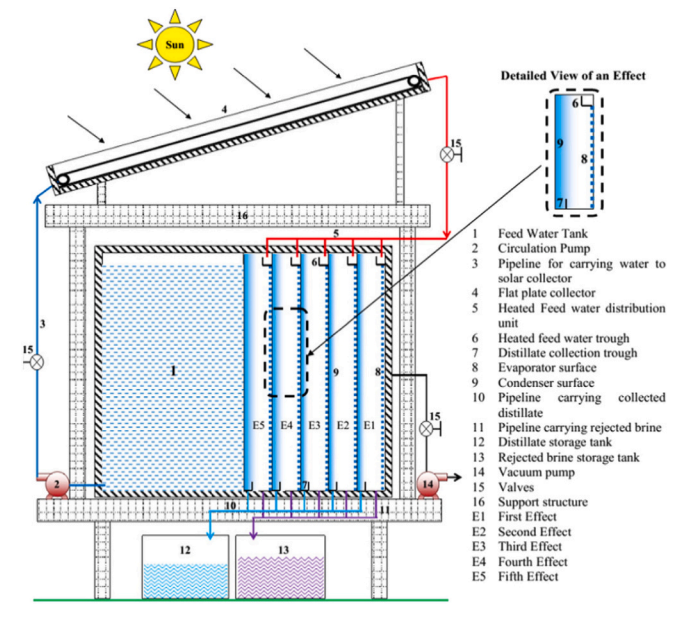


Fig. 17. Schematic of VMED with a solar collector and a vacuum pump [42].

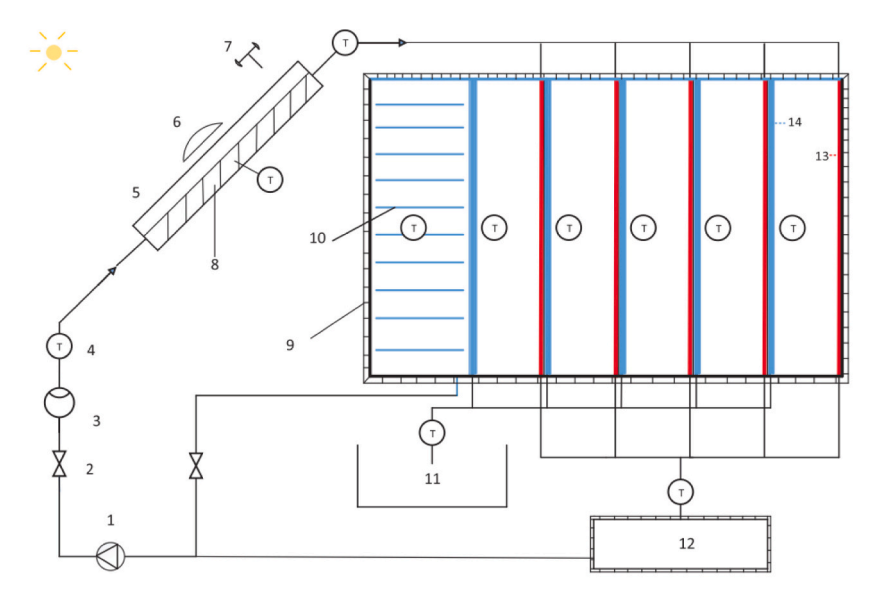
collector is also included in this category of heat sources, such as industrial waste heat, geothermal heat, and biothermal heat.

Elsayed et al. [44] focused on the effect of the inlet temperature of feed water  $(T_f)$  and the feed rate to still  $(\dot{m}_f)$  for a 3-effect VMED with an external heating source (Fig. 19). The VMED comprised intermediate plates inserted between a heating plate and a cooling plate. Heat sources heated the heating plate (or first plate), and the cooling plate was cooled using cooling water. They developed a numerical model of VMED and verified it by its comparison with the experimental results of the 3-effect VMED. Their study concluded that 1) an increase in  $\dot{m}_f$  reduced PR and 2) an increase in the heating water temperature or a decrease in the cooling water temperature improved the PR.

In 2001, Gräter et al. [45] experimentally investigated a 4-effect VMED with heating and cooling loops in their laboratory of Germany. As shown in Fig. 20, the experimental unit comprised a heating loop, a cooling loop, and the 4-effect VMED between the two loops. The VMED had an evaporation area of 1.7 m<sup>2</sup>. To guarantee that the wick adhered properly to the evaporation surface, the VMED was reversely tilted by  $\sim 3^{\circ} - 5^{\circ}$  from the vertical line. The following operation modes and configurations were examined: 1) heat recovery, 2) natural and forced convection in the effects, and 3) intermediation screen. Two blowers were installed to force the convection in the distillation effect to increase the mass transfer. Furthermore, the intermediate screens installed inside the distillation effects separated up-and-down flows and reduced useless energy transport by thermal radiation. The results showed that heat recovery from brine and distillate had a minor influence on the distillate output, while PR increased considerably. Blowers and intermediate screens increased the distillate yield and PR by more than 50% and 60%, respectively, when compared with the case without heat recovery. The distillate output increased strongly with the inlet temperature from the heating loop to the first effect. The equipment produced freshwater with a maximum of 6.1 kg/(m<sup>2</sup>·h) at an inlet temperature of 96 °C with  $Q_{in}$  =

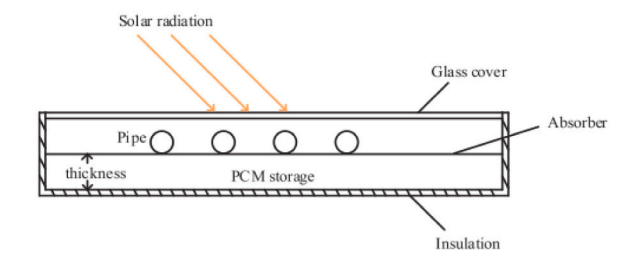
In 2005, Nosoko et al. [46] theoretically studied the effects of boiling point elevation (BPE) of the feed water due to salt concentration on a VMED (Fig. 21). The VMED was equipped with heat exchangers for heat recovery from hot concentrate and distillate leaving the still. The still had a thin heating box for supplying steam at the center and symmetrically arranged two series of effect plates at both sides of the box. They proposed a 2D numerical model to analyze seawater concentration and temperature changes in the vertical direction. Steam at 100 °C was supplied to the first plate of this still, and the last plate was cooled in 30 °C ambient air. Besides, the VMED was installed with heat exchangers for heat recovery from hot saline water and distillate, leaving the still. The numerical results showed that BPE increased more rapidly at downstream distances close to the exits of the evaporating areas, and this BPE increase considerably reduced the evaporation flux downstream of the wicks. Decreasing heat flux and evaporation efficiency resulted in a considerable decrease in the evaporation flux at the midstream and downstream regions on all the wicks. Further, reducing d increased the production rate. They found that the 19-effect VMED with d = 5 mm, and 80% heat recovery could obtain a 13.2 kg/(m<sup>2</sup>·h) for

In 2011, Park et al. [47,48] designed VMED using the waste heat of the exhaust gas from a portable electric generator (Fig. 22). They believed that the waste gas of the electric generators commonly used in many remote areas was hot enough to be used as a heat source for the small-capacity distillers. The exhaust gas from the generator flowed into the copper tubes in the evaporation chamber where water was heated to evaporate and then, the evaporated vapor was condensed on the front side of the first plate. Experimental results showed that the distiller produced at least 6.7 and 6.80 kg/d of distilled water with a single- and 2-effect still, respectively. This amount corresponded to 19.4–25.0 kg/d for a 10-effect VMED, which was estimated from a previous study [39]. VMED was effective when the operating time of the portable engine



1.Pump 2. Gate Valve 3.Flow Meter 4.Sensor Temperature 5.Collector 6.Pyranometer 7.Anemometer 8.PCM
 Storage 9.Insulation 10.Saline Storage 11.Distilled Water 12. Water Storage 13.Saline Water 14.Condensing
 Path

## (a) VMED with a solar collector



## (b) Solar collector with the PCM at the back of the absorption plate

Fig. 18. Schematic of VMED with a solar collector and a PCM [43].

generator was more than 3 h.

In 2016, Seleem et al. [49,50] studied a single-effect VMED with hot and cold water sprays in Cairo, Egypt. As shown in Fig. 23, a test system was set up to assess the performance and evaluate the productivity of the stills with both flat and folded effect plates. A numerical model was developed for VMED. The folded plate was fabricated with a chevron-shaped surface (Fig. 24). It was found that five parameters influenced the productivity of the still: the hot plate temperature, mass feed rate, d, cold plate temperature, and  $T_f$ . Two of the parameters, the hot plate temperature and  $m_f$  considerably influenced the performance of the still. The productivity increased when the hot plate temperature increased and  $m_f$  decreased. The experimental results showed that the production was 7.158 and 3.0 kg/( $m^2$ ·h) for the chevron-shaped and flat plates, respectively.

In 2016, Tanaka [51] proposed VMED that employed the thermal energy from biomass burned in a stove during cooking (Fig. 25). The thermal energy from the stove was transported to the VMED through a heat pipe. After the biomass began to burn, the combustion chamber temperature increased to  $\sim\!600\,^{\circ}\text{C}$ , and the heat plate temperature of the distiller increased to  $\sim\!90\,^{\circ}\text{C}$ . An experimental apparatus was fabricated and tested using single- and multiple-effect distillers to investigate whether a heat pipe could transport thermal energy adequately from the stove to the distiller. Test results showed that the heat plate and first partition temperatures of the distiller reached  $\sim\!100\,^{\circ}\text{C}$  and  $90\,^{\circ}\text{C}$ ,

respectively, at a steady-state, indicating that the heat pipe worked sufficiently. The water production was about 0.75 and 1.35 kg during the first 2 h using the single- and 4-effect VMEDs, respectively.

Previous studies on VMEDs with external heat sources have been mainly conducted in two directions. First, for studying the performance characteristics of the VMEDs, which is not applicable for practical purposes but to study how various variables affect the performance of a distiller, second, for easily accessing a heat source in the fields. It is interesting to evaluate the operability and productivity of VMEDs when heat sources such as waste heat or biogas heat are used.

## 5.4. VMED with a reflector

Studies have been conducted to increase production using reflectors in various types of solar distillers [52], which is an effective strategy to improve performance because it can simply increase solar radiative absorption using easily accessible materials such as a flat plate, mirror, and film.

In 2005, Tanaka and Nakatake [53–56] designed VMED coupled with a flat mirror (Fig. 26). They installed a flat mirror as the radiation reflector below the front plate to absorb reflective solar radiations into the first plate. Besides, a selective absorbing film was attached to the front surface, which increased the absorption rate of solar radiation, and the first partition was covered with glass at an interval of 10 mm for

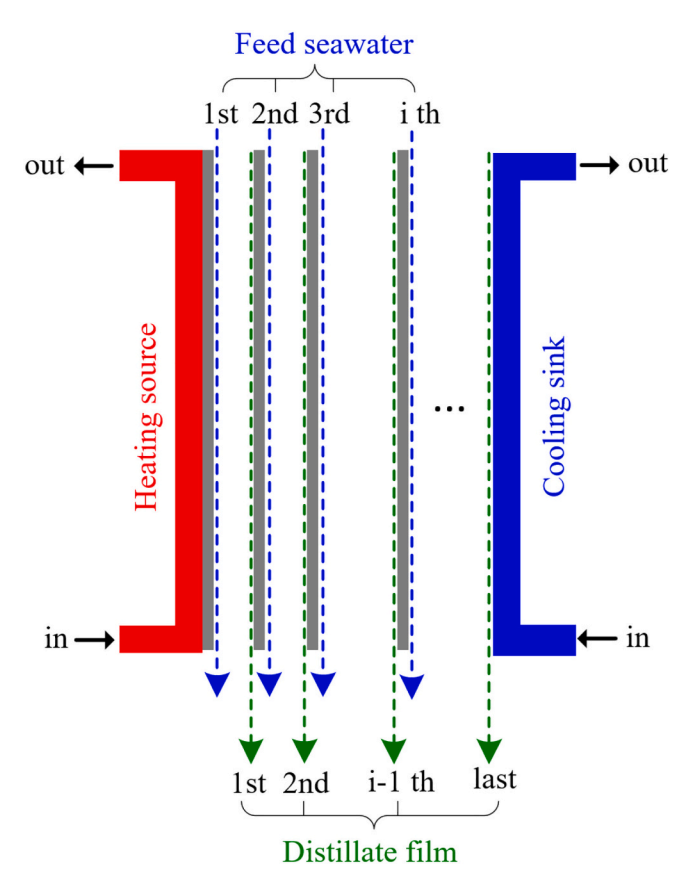


**Fig. 19.** Schematic of VMED with constant temperatures in the heating source and cooling sink.

insulation. The angle of the mirror could be altered to increase the solar radiation absorption rate for the front plate. Further, the three casters installed below the VMED and reflector were allowed to rotate the still to orient it toward the sun during the day. First, they designed a numerical model and estimated the effects of various parameters on the productivity of VMED [55,56]. They found that the absorption of solar radiation in the first partition was considerably increased by rotating the still at the southing of the sun just once a day, and the optimum angle of the flat-plate mirror was  $15^{\circ}$  and  $8^{\circ}$  on a spring equinox and the winter

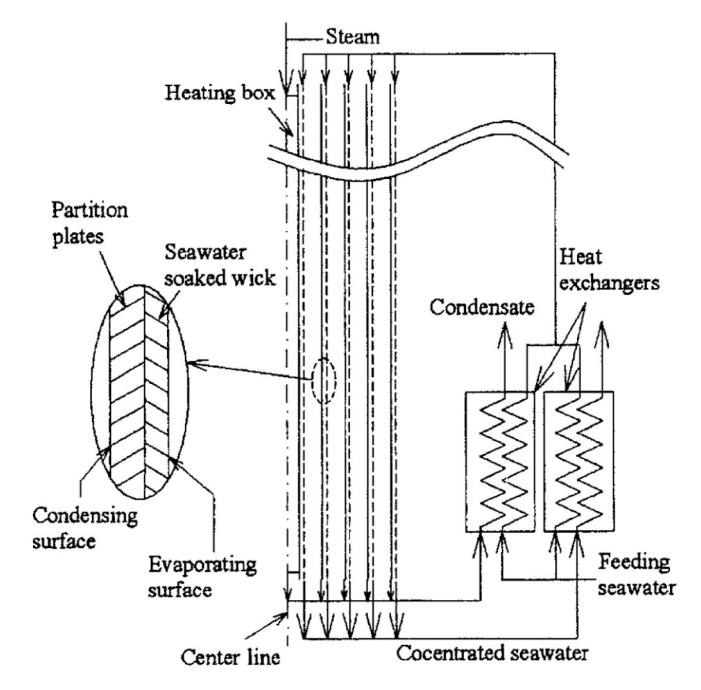


Fig. 21. Schematic of VMED heated by steam [46].

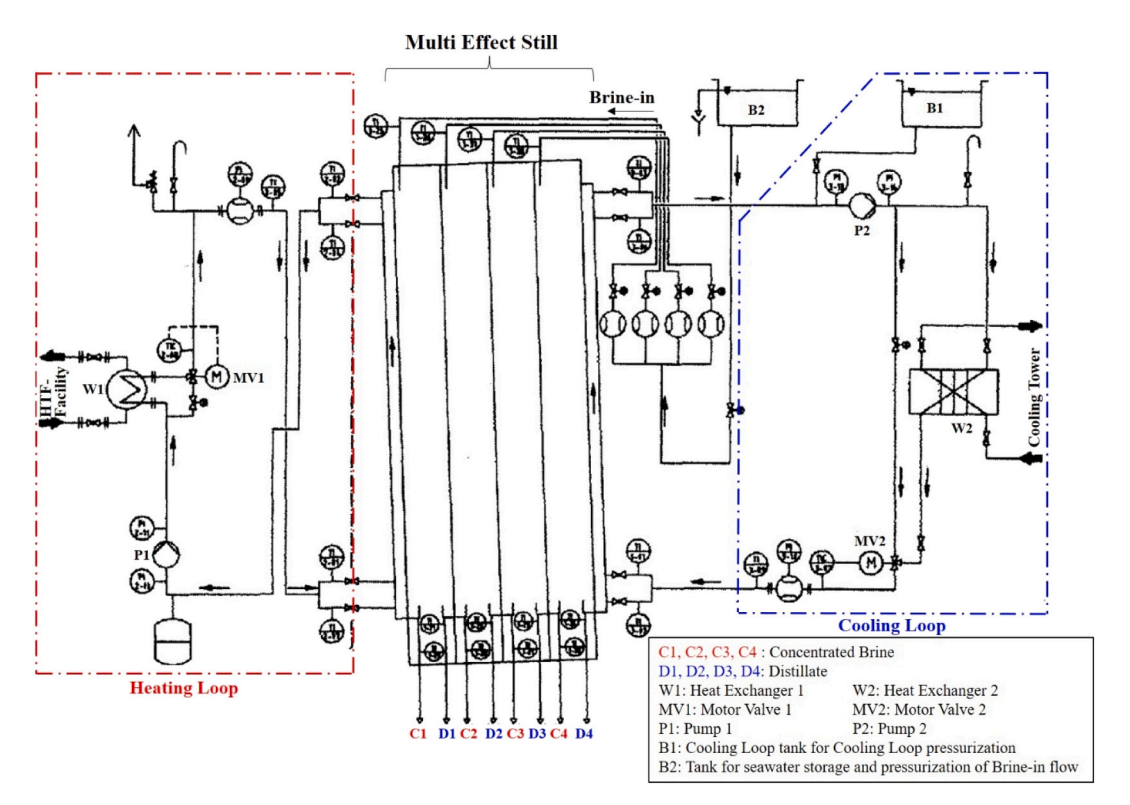


Fig. 20. Schematic of 4-effect VMED with heating and cooling loop [45].

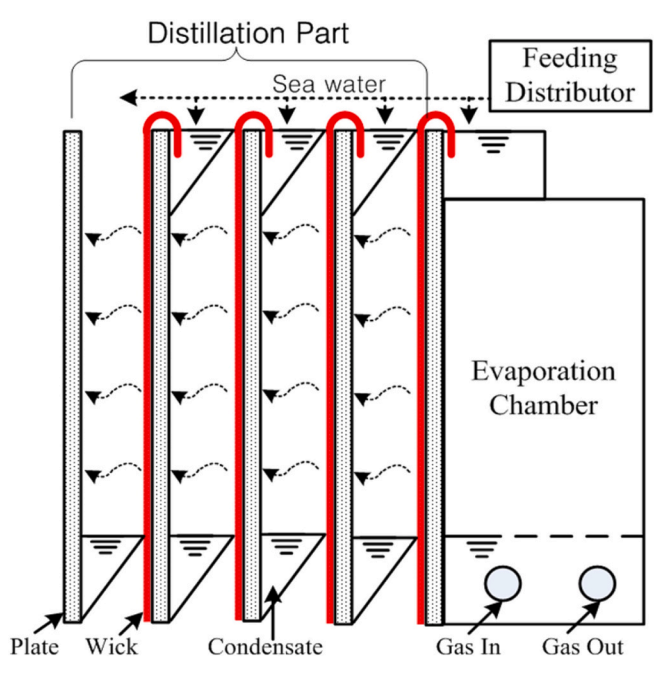


Fig. 22. Schematic of VMED using waste heat [47].

solstice day, respectively, at the equator. A 10-effect VEMD with d=10 mm was predicted to produce 29.2 and 34.5 kg/( $m^2$ ·d) on sunny spring equinox and winter solstice days, respectively at the equator [55].

In a subsequent parametric study [56], the results showed that  $m_d$  decreased by  $\sim$ 15% with an increase in d from 5 to 10 mm or a 1.5 times increase in  $\dot{m}_f$ . The most effective angle of the flat-plate reflector was  $\sim$ 10° throughout the year. The  $m_d$  of the proposed still with 10 partitions under practical conditions was predicted to be  $\sim$ 18.0 and 21.5 kg/( $\rm{m}^2$ ·d) on the spring equinox and winter solstice days, respectively, at the equator.

In 2007, Tanaka and Nakatake [53] performed a theoretical analysis to determine the optimum angle of the flat plate reflector and the optimum azimuth orientation of the still throughout the year at the equator and at  $10^{\circ}$ ,  $20^{\circ}$ ,  $30^{\circ}$ , and  $40^{\circ}$  northern latitude. Values of azimuth

orientation for east, south, west, and north is  $-90^\circ$ ,  $0^\circ$ ,  $90^\circ$ , and  $180^\circ$ , respectively. Numerical results showed that the flat-plate reflector's angle should be fixed at  $10^\circ\mathrm{E}$  and changed to be  $0^\circ\mathrm{E}$  during the winter season at high latitudes. The optimum azimuth orientation of the still was the smallest in winter and largest in summer.  $m_d$  was predicted to be in the range of 30--38 kg/(m²·d) throughout the year at any latitude except during the winter season at  $40^\circ\mathrm{N}$  latitude. Finally, they performed outdoor experiments for VMED [54]. The results showed that the  $m_d$  of the 10-effect VMED with a reflector was  $\sim 5$  or 6 times that of a single-effect still.

Despite the reflector's benefits, all the studies were conducted only by a Japanese research team. Studies on VMED with reflectors need to develop simpler and more efficient designs for various locations. Integrating the classical VMED with a reflector can become an exciting research topic.

#### 5.5. VMED with a basin

The CSS is a standard model in solar stills due to its stability,

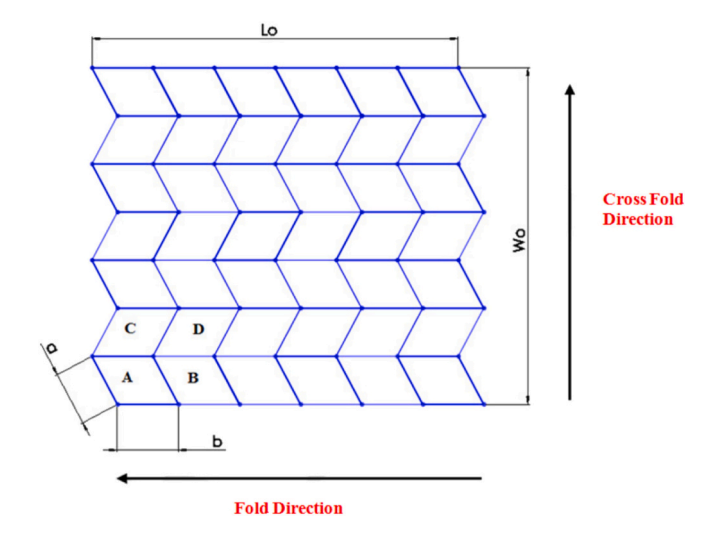


Fig. 24. Top view of the chevron pattern for the folded plate [49].

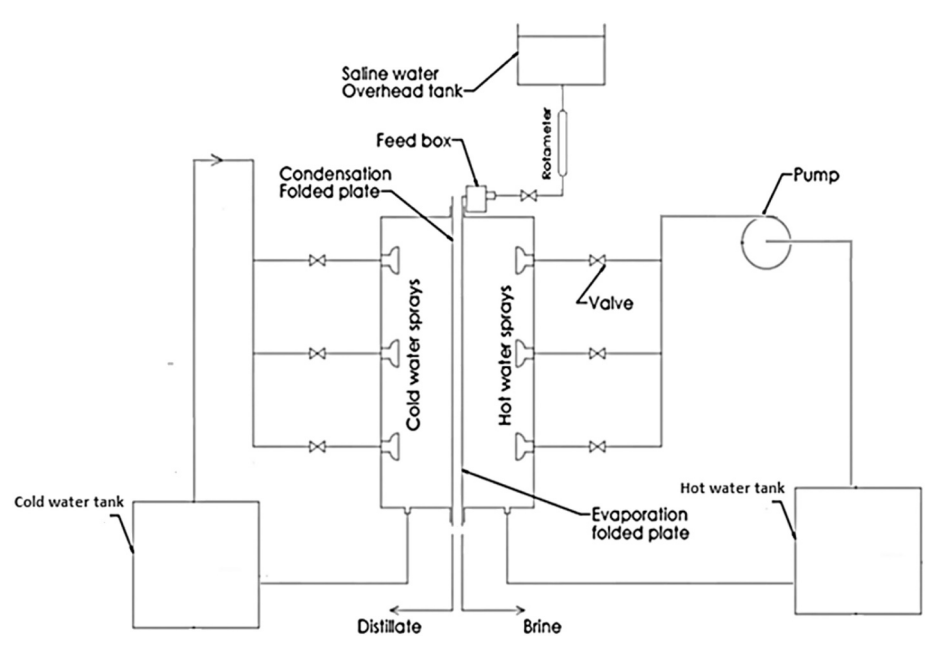


Fig. 23. Schematic for the test of single-effect VMED with cold and hot water sprays [49].

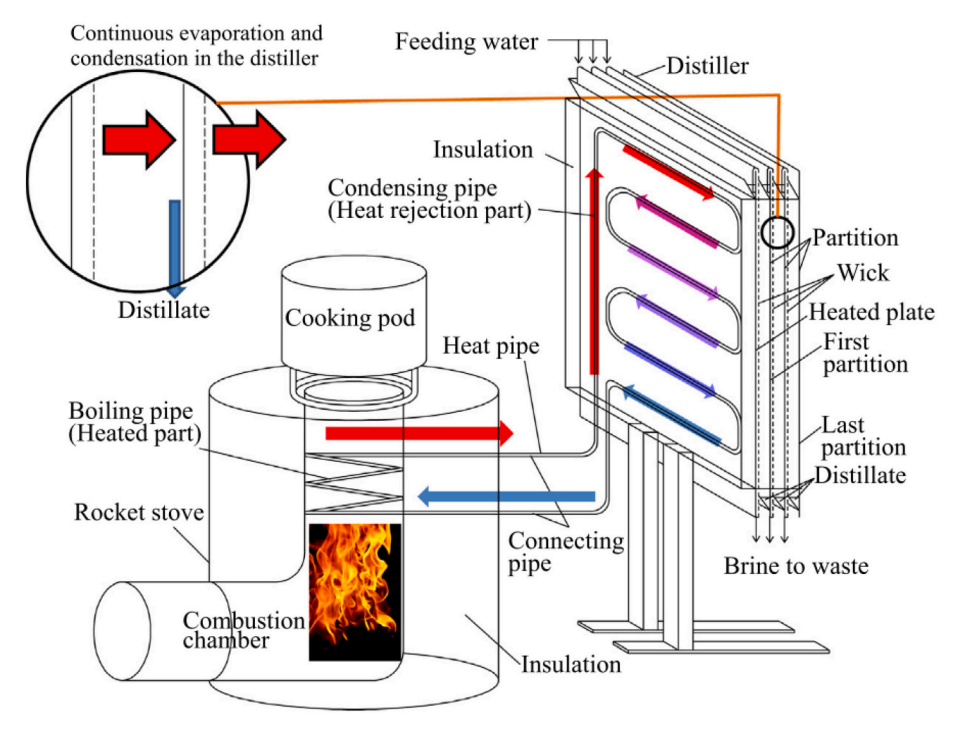


Fig. 25. Schematic of VMED using biomass energy [51].

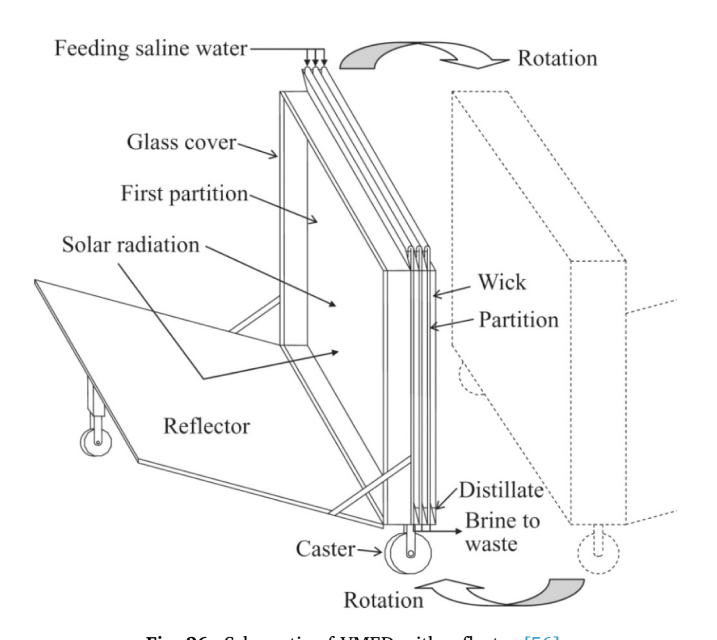


Fig. 26. Schematic of VMED with reflector [56].

simplicity, and reliability. Multiple-effect distiller can afford more freshwater effectively. Therefore, the advantages of the two distillers can be realized by combining them.

In 2000, Tanaka et al. [57] designed the first VMED with a basin (Fig. 27). The VMED comprised a single-slope basin section and a vertical multiple-effect section attached with the basin section's back wall. The basin section comprised a sloping double glass cover, a horizontal basin liner, and triangular sidewalls. The double glass cover with a narrow air gap reduced thermal losses through glass cover such that a considerable portion of the basin thermal energy was transferred toward the multiple-effect section. The first plate (back wall of the basin) of the multiple-effect section got multiple thermal energy such as the latent heat by condensing vapor, the heat transferred by convection from the hot basin air, and direct solar radiation. The still could produce

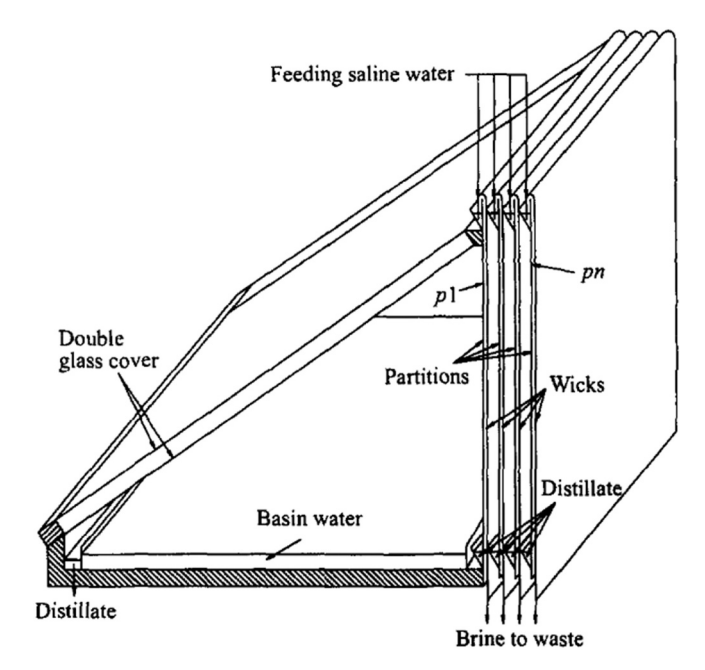


Fig. 27. Schematic of VMED with a basin [59].

freshwater at the cover glass and back wall in the basin section as well as the multiple effect section. In this review, the distillate from the basin's back wall is considered for determining production in the basin section; therefore, we define the distiller presented in Fig. 27 as 3-effect VMED, not 4-effect VMED. Tanaka et al. [57] developed the numerical model for the VMED with a basin to analyze the performance and characteristics. The numerical study showed that the still with d=5 mm had  $m_d=15.4$  kg/(m²·d) at 22.4 MJ/(m²·d) solar radiation, and the cumulative efficiency was ~3.5 times greater than that of the CSS. Additionally, they performed a numerical study [58] for determining the effects of three design parameters and two operational parameters on the productivity of distillate for the proposed still on sunny days for four

seasons. The considered parameters were the angle between the glass cover and horizontal basin, d,  $N_b$ ,  $m_f$ , and the initial saline water mass in the basin. The numerical results showed that the productivity of a 13-effect still with d=5 mm and a  $40^\circ$  angle of the glass cover was four times greater than that of the CSS, and was  $\geq \sim 40\%$  for the classical VMED. Productivity was higher in autumn than in spring because of the higher  $T_{amb}$  at similar solar input energy. Productivity exponentially increased with a decrease in d and an increase in  $N_t$ . Increasing  $m_f$  decreased the productivity in all seasons. The productivity gradually decreased with an increase in the initial saline water amount in the basin.

In 2002, Tanaka et al. [59] performed an experimental study for an 11-effect VMED with a basin. Results showed that the still with d=5 mm produced 14.8–18.7 kg/d per unit effective area of the glass cover at  $Q_{gls}=20.9–22.4$  MJ/(m²·d) and  $T_{amb}=19–30$  °C. However, they warned that the contact between the wick and condensing surfaces due to thermal stress of the partitions and wind force reduced the output. Therefore, they recommended using nine small spacers in every diffusion gap between the effect plates.

Park et al. [60,61] and Yeo et al. [62] in South Korea studied VMED with a basin that could use waste as the heat source (Fig. 28). Their distiller was similar to the equipment shown in Fig. 27 but had a heat exchanging tube in the basin liner to recover waste heat, providing hybrid heat sources to the distiller. This still had the advantage of being able to operate using a single heat source of either solar energy or waste heat or using both heat sources simultaneously. Further, the internal reflecting fins attached to the heat exchange tube functioned as the reflectors of the solar radiation energy to the back wall as well as the heat transfer augmentation fins of the tube. They used the waste heat from an electric generator based on a previous study [48]. In 2015, an experimental study by Park et al. [60] showed that a 2-effect VMED with a basin produced a maximum of 21 kg/(m<sup>2</sup>·d) at 5800 kJ/h (1.61 kW/m<sup>2</sup> based on the collecting area of 1 m<sup>2</sup>) of waste heat only, and PR was 14.8-16.9. In addition, performance tests [61] were performed with three operational parameters: the amount of waste heat input,  $\dot{m}_f$ , and the seawater level in the basin. Experimental results showed that  $m_d$ linearly increased with a heat input, affording 18.02 kg/(m<sup>2</sup>·d) at  $Q_{in}$  = 22.37 MJ/( $m^2$ ·d). The maximum  $m_d$  was obtained at the lowest basin water level. They found that there existed  $\dot{m}_f$  to obtain the maximum productivity at a given heat input, and the MED section played a more critical role than the basin section for improving the performance of the VMED with a basin.

In 2019, Yeo et al. [62] studied the effects of three heat sources (solar thermal energy, electric heater, and waste heat) on the performance according to design and operating parameters in VMED with a basin

(Fig. 28). The parameters were insulation on both glass sidewalls, reflecting fins inside the basin, the initial level of the seawater in the basin, and  $m_f$ . The experimental results showed that the effect of the thermal insulation on both sidewalls in the basin section had a greater effect on the freshwater production using solar energy (16.7%  $\uparrow$ ) than while using waste heat (5.3%  $\uparrow$ ) and that the internal reflecting fins decreased the productivity. Furthermore, regardless of the type of heat source, lowering the initial level of seawater in the basin increased productivity; however, an optimum depth existed (5 mm for solar energy at  $Q_{glb} = 20.62 \, \text{MJ/(m}^2 \cdot \text{d})$  and 15 mm for waste heat at 23 MJ/m²). PR of the still was the lowest for solar energy (0.18–0.71) and the highest for waste heat (2.32). Although the optimum  $m_f$  increased with the amount of heat supplied, the optimum ratio,  $m_f/m_e$  was in the range of 4.6–2.8, regardless of the amount of input energy.

Kaushal et al. [63] designed a 3-effect VMED with a basin in which a floating wick was applied (Fig. 29). The feed water of this still was preheated by recovering heat from hot wastewater. The experimental results showed that the  $m_d$  of the still with a floating wick was 21% higher than that of the still without the wick and higher at night due to the extra heat stored in the floating wick as well as reduced radiative and convective heat losses. In addition, they found that when the still was operated for an entire day, the salt in the wicks was largely flushed during the night due to no evaporation and no salt deposition.

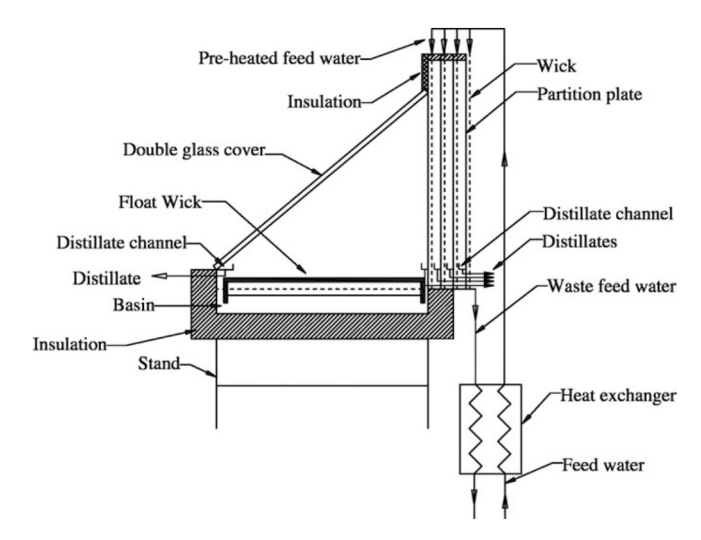


Fig. 29. Schematic of 3-effect VMED with a basin and a floating wick [63].

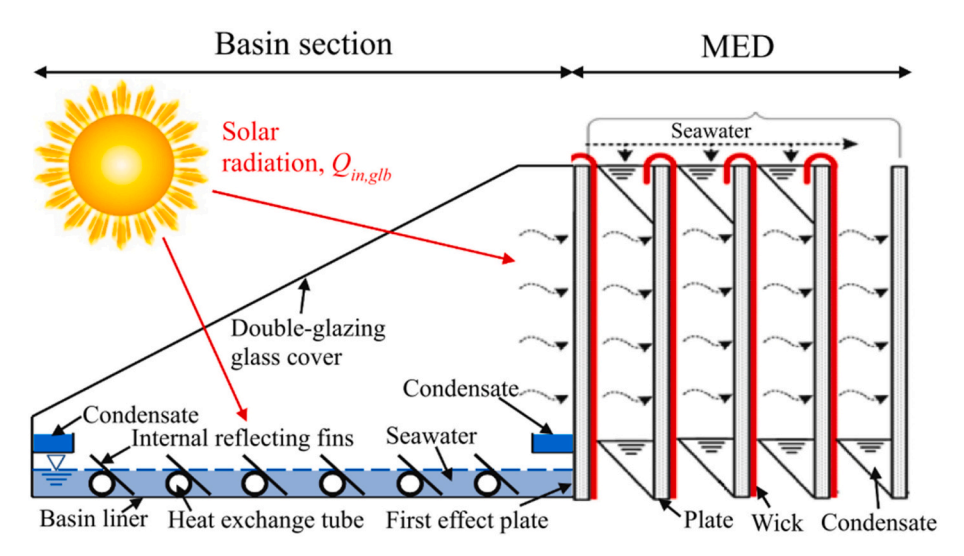


Fig. 28. Schematic of VMED with a basin and involving waste heat and solar energy as heat sources [62].

In 2018, Dhindsa and Mittal [64] developed a 3-effet VMED that incorporated a basin integrated with a mini solar pond for generating nocturnal freshwater (Fig. 30). They installed a mini solar pond (Fig. 31) with a reasonably large thermal storage capacity to store solar energy during the day and produce freshwater during the night by supplying the thermal energy stored during the day from the pond to the distiller. As shown in Fig. 31, the trapezoidal shape of the pond mitigated the shading effect of the sidewalls, and a reflector above the pond was used to enhance solar intensity. The still had multiple floating wicks in the basin that were prepared by wrapping blackened porous cotton cloth on the basin water surface. At Thapar University in Patiala, India, they compared their distiller with the conventional basin-VMED under the same conditions. Experimental results showed that the modified VMED's diurnal, nocturnal, and overall total productivity was 49.87%, 71.21%, and 56.92% higher than those of the conventional basin-VMED, respectively. The cumulative daily efficiency of the modified VMED and conventional basin-VMED was 80.29% and 59.6%, respectively, when the total solar radiation on the glass cover was 23.1  $MJ/(m^2 \cdot d)$ .

In 2015, Sharon and Reddy [65] presented a single-effect VMED with an upper basin (Fig. 32). The overhead basin served as a reservoir of feedwater storage and a preheater for the feed water. This still had only a single effect but could produce the distillate from both sides. They designed two types of the upper basins: single- and double-slope types. The still received solar radiation from both east and west directions. The results showed that the still with the double-slope basin produced more distillate than that with a single-slope basin. The maximum  $m_d$  for the still with a double-slope basin was 6.015 kg/( $m^2$ ·d) for April, and the thermal efficiency was in the range of 36.22%–58.01%.

## 5.6. VMED with a curved-plate

In 2014, Chong et al. [66] presented a VMED with a bent plate to address the wick's peel-off and heating plate deformation issues (Fig. 33). They believed that the bending structure increased the strength of the plates when using plastic material such as polycarbonate as the heating plate [Fig. 33(b)], and the wick material was stretched to generate a tensile force for tight contact with the bent plate. The distiller was powered by a vacuum-tube solar collector, and feed water was distributed uniformly to all wicks through a 5-cm-thick pulp sponge on the top of the plates. The solar energy absorbed by the vacuum-tube collector was transferred to the first plate via a thermosyphon loop.

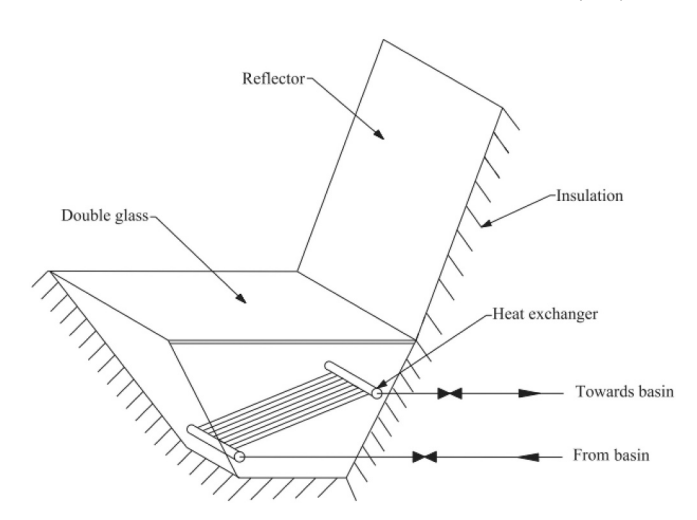


**Fig. 31.** Schematic of a trapezoidal mini solar pond with a heat exchanger [64].

The test results showed that the highest  $m_d$  was 23.9 kg/(m<sup>2</sup>·d) based on the unit area of the glass cover, and PR was 1.5–2.44 at  $Q_{glb} = 22.1$  MJ/(m<sup>2</sup>·d).

In 2015, Xie et al. [67] developed a 3-effect VMED with a cylindrical shape (Fig. 34). Although this distiller was also included in the group of VMEDs with a solar collector described in Section 5.2, it was classified as the VMED with a curved plate because we wanted to emphasize the unique shape of the effect plate. The proposed still had the characteristics that the cylindrical effect plates had corrugated surfaces with transverse ridges, and the water troughs on the ridges replaced the porous wick. The ridges increased the heat transfer area between the vapor and seawater in the troughs. In contrast to the other VMED with a solar collector, thermal energy from the collector was transferred to the chamber center of the cylindrical VMED to decrease the heat loss from the still. The still had an effective collection area of 1.48 m<sup>2</sup>. The total condensation area was 3.51 m<sup>2</sup>, which was three times larger than the evaporation area. Test results indicated that PR was 1.35 in solar conditions, and the maximum PR was 1.81 for steady-heating power. This VMED produced 6.9 and 1.6 kg of freshwater during the day and at night, respectively.

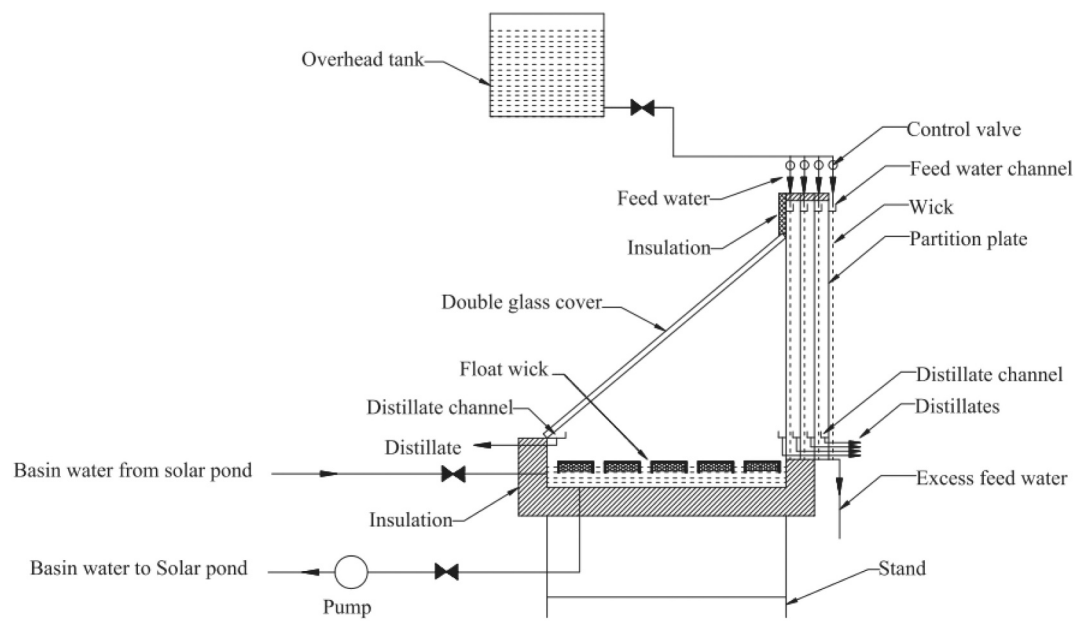


Fig. 30. Schematic of 3-effect VMED with a basin integrated with mini solar pond [64].

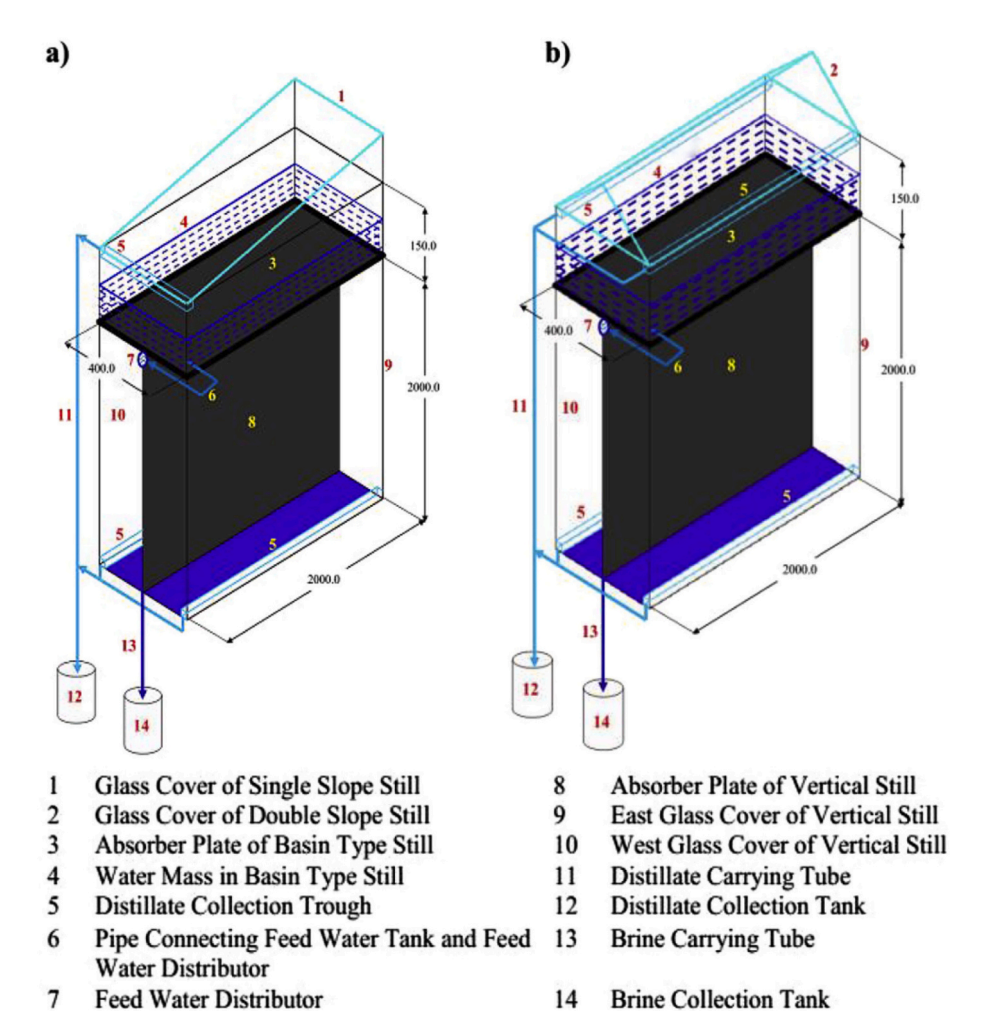


Fig. 32. Schematic of single-effect VMED with upper basin: a) single-slope basin b) double-slope basin [65].

In 2015, Huang et al. [68] constructed a 14-effect VMED with spiralshaped effects (Fig. 35). The effect plate (made of polycarbonate) and wick were spiraled together at the bottom and top edges using two rectangular spacers. The still had a single spiral continuous gap between the first heating section (or center) and the cylinder's exterior. Because the vapor could diffuse freely and laterally down to the end of the effect, thermal and mass transfer processes were improved at a high-heat input. The bottom silicone rubber spacer also served as a ditch for collecting freshwater. During the manufacturing process of rolling the plate, the wick was stretched on the curved plate using a tensile force similar to a previous study [66]. The ditch below the plate was placed to collect the distillate. Heat recovery pipes were connected with VMED to recover the thermal energy contained in the fresh and brine water. The vapor generated by the vacuum-tube solar collector was transferred to the condenser at the center of VMED through a thermosyphon loop (Fig. 35). The test results showed that the highest production was 40.6 kg/d (34.7 kg/(m<sup>2</sup>·d) based on the glass cover area), and PR was in the range of 2.0–3.5 under  $Q_{gls} = 24.9 \text{ MJ/(m}^2 \cdot \text{d})$ .

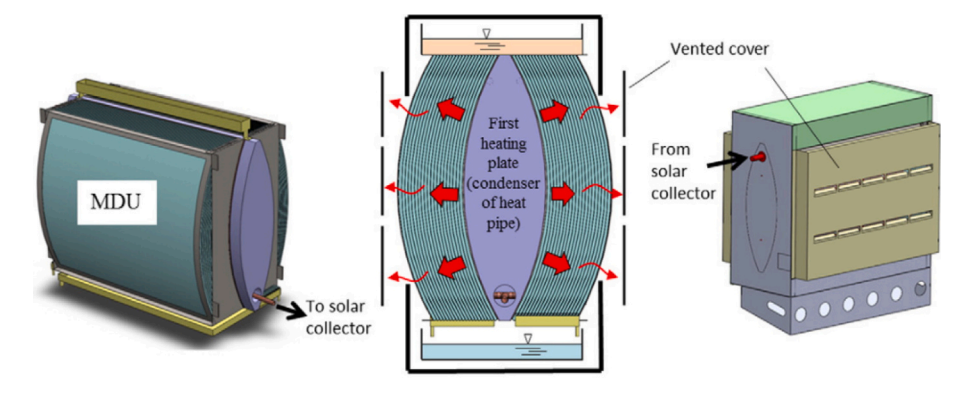
In 2020, Huang et al. [69] developed a 6-effect VMED with a cylindrical plate (Fig. 36). The shape of this distiller was similar to the cylindrical VMED developed by Xie et al. [67], but they applied a wick instead of troughs on the evaporating surface. The multiple cylindrical effects comprised a series of copper tubes with equal incremental radii, arranged in a concentric configuration. In the solar thermal concentrator installed above VMED, the disk-shaped solar collector absorbed the solar energy in a vacuum and then transferred the energy to a copper rod welded with a disk. The thermal energy of the rod, which was placed at

the center of VMED, was transferred to the effect plate. A water bath cooled the last plate at 25 °C. In an indoor experiment, they used a solar simulator to provide steady heat flux, and the results indicated that the water production was  $2.2 \, \text{kg/(m}^2 \cdot \text{h})$  in the VMED under a solar intensity of  $1 \, \text{kW/m}^2$  under thermal concentrations of three suns. Besides, the outdoor tests on the rooftop demonstrated that  $m_d$  was  $3.9 \, \text{kg/(m}^2 \cdot \text{d})$  at a low solar intensity of  $415 \, \text{W/m}^2$ .

## 5.7. VMED with a tilted wick still

CSS has a drawback when the diffusion distance of vapor is long. However, the tilted wick still has a structure such that the diffusion distance is shortened. VMED with a tilted wick still can increase efficiency and reduce the device size compared with the VMED with a basin.

Tanaka [23,70,71] designed a VMED integrated with a tilted wick still. The VMED comprised a tilted wick section and a multiple-effect section (Fig. 37). The author tried to improve VMED with a basin still (refer to Section 5.5), which was too bulky for easy transportation. The tilted wick section was similar to the basin-type solar still and comprised a double glass cover and a wick. The wick acted as a basin and a solar absorber. Vapor evaporated from saline water was diffused and condensed on the inner glass cover. Further, the vapor moved to the first plate via natural convection, condensed on the surface of the first plate, and then transferred latent heat. In 2016, Tanaka [23] developed a numerical model and analyzed the characteristics of the VMED with a tilted wick still. The results showed that  $m_d$  was predicted to be approximately 19.2, 16.0, and 15.9 kg/( $m^2$ ·d) on the spring equinox,



## (a) Configuration of VMED with a bent-plate



(b) Bended PC plates

Fig. 33. VMED with bent plates [66].

Afterward, Tanaka [70] performed a parametric study for VMED. The parameters were the inclination angle of tilted still, the ratio of the height of VMED to the length of tiled still, air gap sizes in double glass covers, d, and  $N_t$ . The author tried to find the optimum value to produce the maximum value of  $m_d$ . The inclination angle of the tilted still was  $\sim 30^\circ$  in all seasons. With optimum conditions, the total daily output of the still would be competitive against the other types of multiple-effect stills. An outdoor experiment using a 4-effect VMED was performed, and it was found that the discrepancy between the experimental and theoretical results was  $\sim 10\%$ .  $m_d$  increased with a decrease in  $\dot{m}_f$ , d, and  $N_t$ . An optimum gap of cover glass in the VMED section and tilted wick still was 20 and 10 mm, respectively. Under optimum conditions, the still produced freshwater with an average of 35.5 kg/(m²-d) in a year. Additionally, in 2017, Tanaka and Koji [71] experimentally investigated

summer, and winter solstices, respectively, when d = 5 mm and  $N_t = 10$ .

The numerical analysis results on VMED with a tilted wick still indicated that the productivity was 2.13 times higher than the experimental results for the VMED with a basin. Nevertheless, further experimental research is required to evaluate the performance of VMED with a tilted wick still in high-insolation conditions. It is difficult to compare the performance of this VMED with the other types of VMED because the experimental results were obtained only in low-insolation conditions. Because this distiller has resolved the disadvantages of the basin, more production can be expected.

the performance of VMED with a tilted wick still in Kurume College,

Japan. The results showed that the maximum  $m_d$  was ~4.88 kg/(m<sup>2</sup>·d)

at  $Q_{glb} = 13.6 \text{ MJ/(m}^2 \cdot \text{d)}$ .

#### 5.8. Horizontal VMED

In 2004, Fukui et al. [72] developed a horizontal VMED for obtaining drinking water when drifting in an emergency at sea (Fig. 38). The top plate of the VMED was covered by a transparent film and a wick attached under the surface of the plate that extended out to the sea to soak seawater via capillary force. The wicks were attached on both sides of all effect plates except for the first top plate. The condensate-soaked wicks of the upper surface were extended into two plastic bags for condensate storage. A numerical study showed that the proposed still produced  $\sim\!15~\text{kg/(m}^2\text{-d})$  on 22 MJ/(m $^2\text{-d})$ .

Because this study was conducted mainly based on numerical analysis, experiments for verification are required. For the horizontal VMED, it should be verified through operation tests whether problems such as bending of plate and seawater drop on horizontal plate occur.

## 6. Comparison of VMED

## 6.1. Research trend according to the types of VMED

Considering the previous studies' trend according to types of VMED (Fig. 39), the study of the classical VMED accounted for 22.45% followed by VMEDs with a solar collector and a basin. Notably, all types of VMEDs have been evenly studied. As shown in Fig. 40, interestingly, considering the latest trend, research on the classical VMED has been in the spotlight again since 2018. Related studies [29,30] argued that sufficient freshwater could be obtained with optimum design and operation without installing additional units. Additionally, studies for

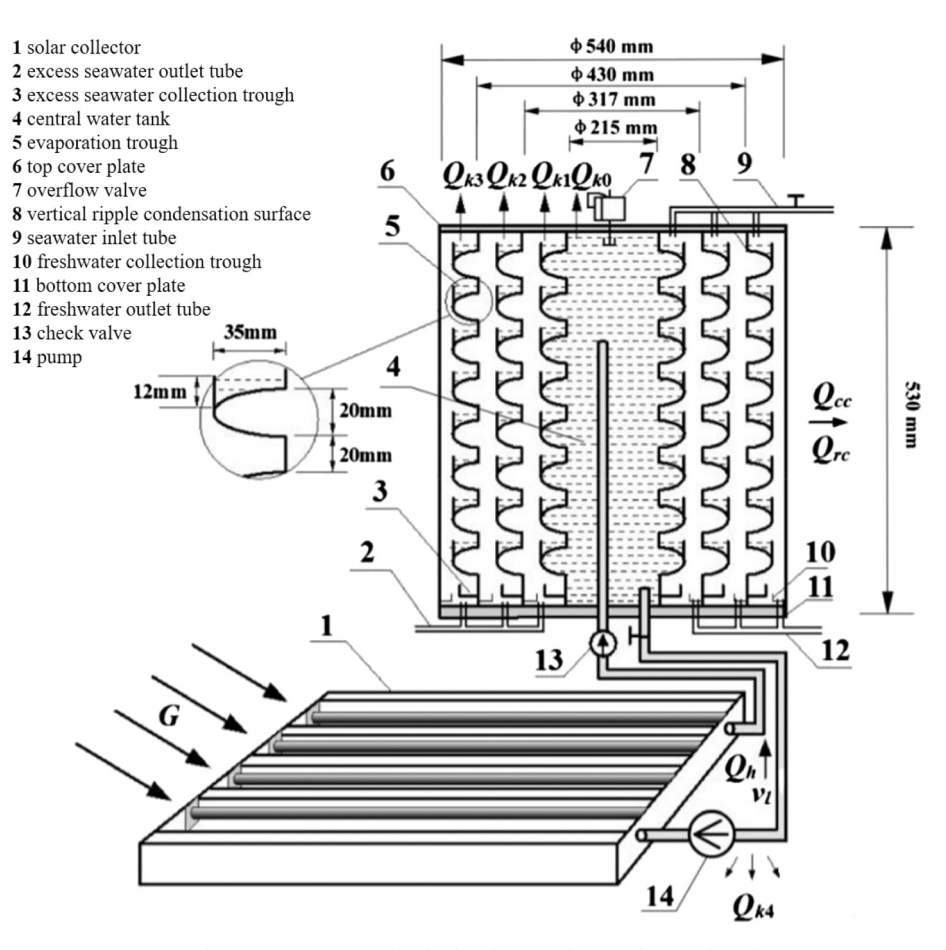


Fig. 34. Schematic of VMED with cylindrical effect plates and vertical ripples [67].

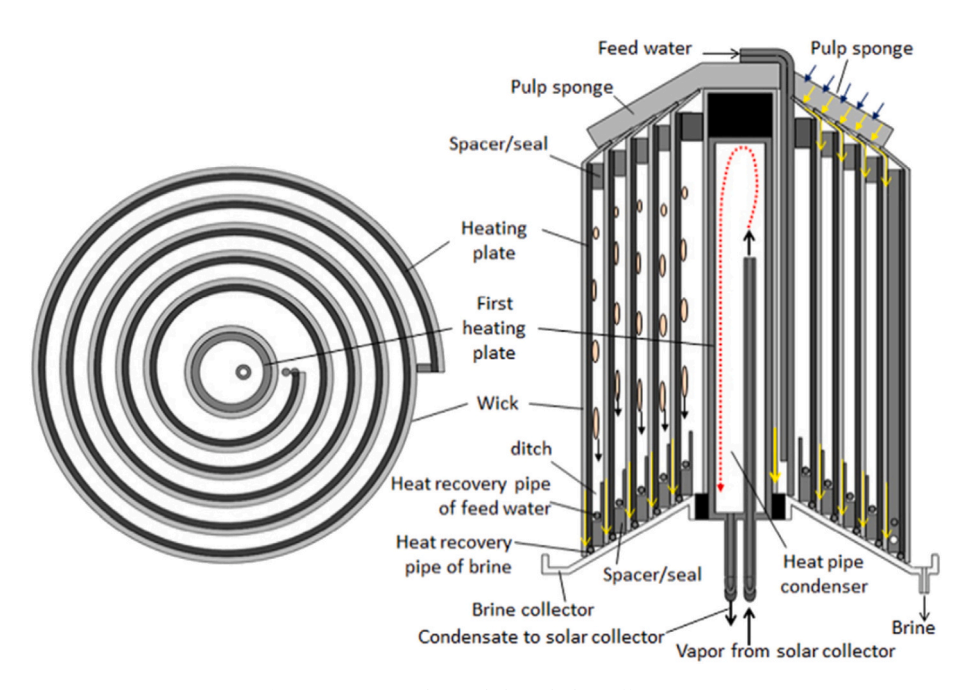


Fig. 35. VMED with spiral-shaped plate effects [68].

VMEDs with a basin, a curved plate, and a tilted wick still are attracting attention as the latest research. However, research on horizontal MED has not been in progress since 2004. Moreover, studies on VMED are still increasing at present, partly due to the increasing demands of renewable

energy.

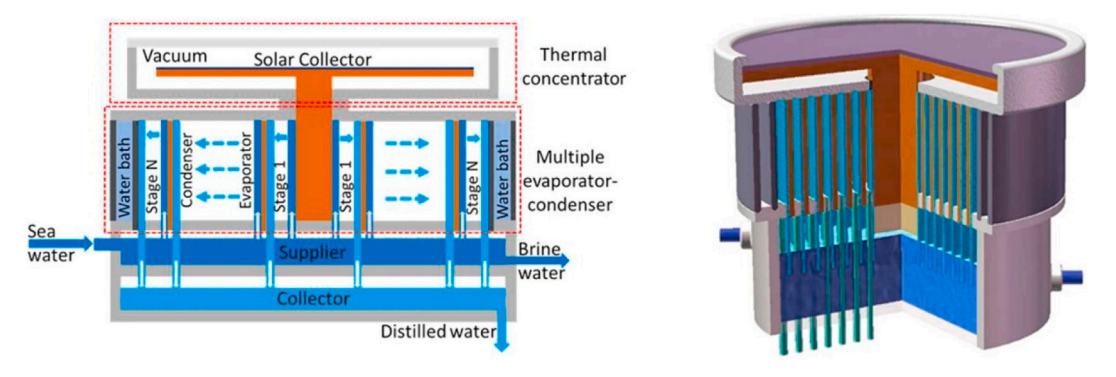


Fig. 36. VMED with cylindrical plate [69].

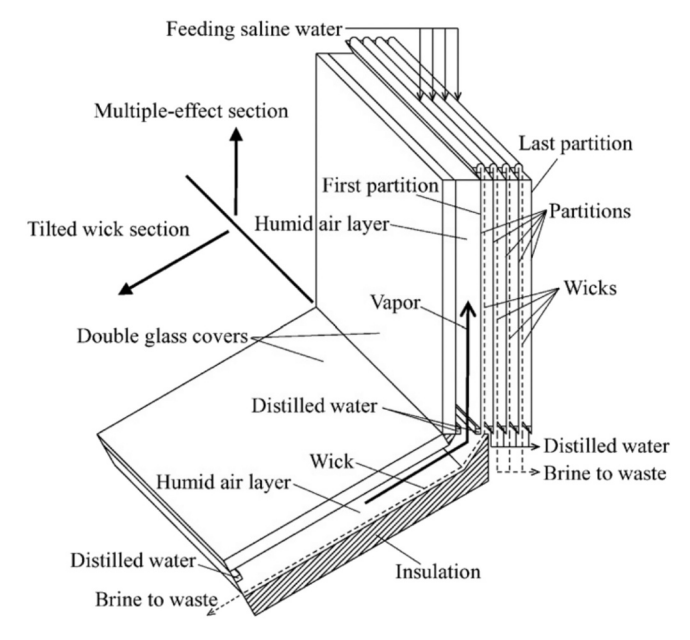
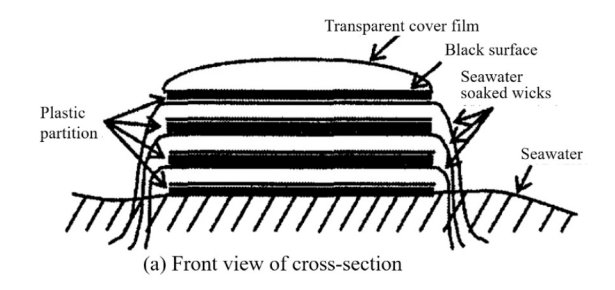


Fig. 37. VMED with a tilted wick still [23].



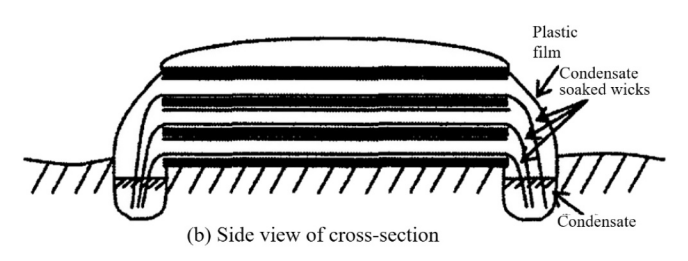


Fig. 38. Horizontal VMED.

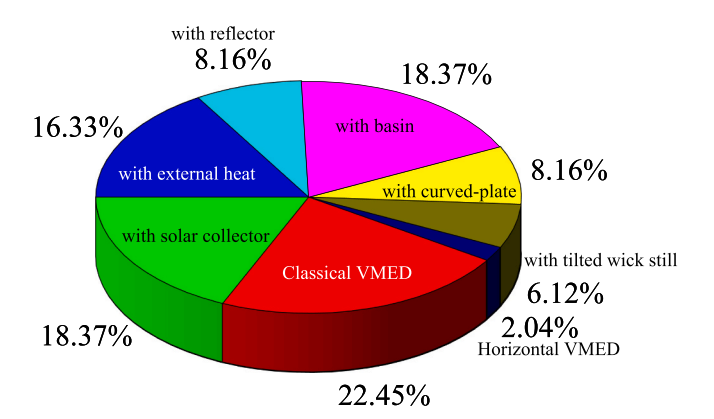


Fig. 39. Percentage of research according to the type of VMED.

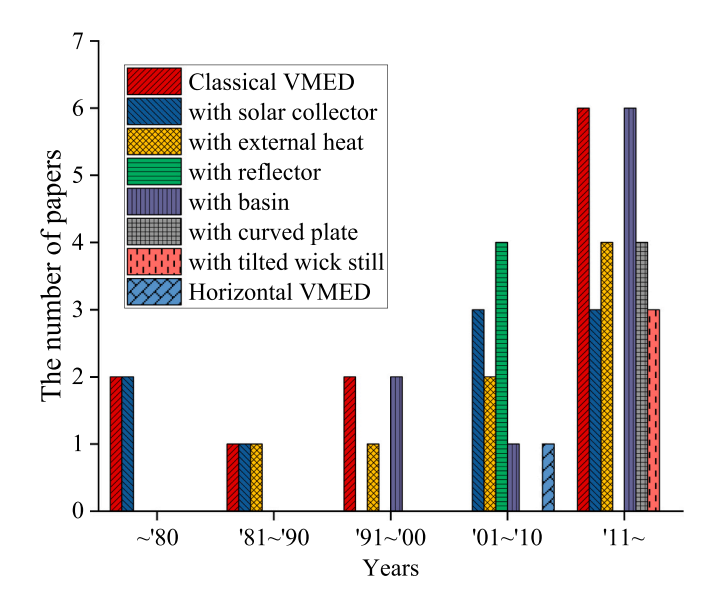


Fig. 40. Number of papers by types of VMEDs.

## 6.2. Performance comparison according to the types of VMED

Table 1 summarizes the freshwater production with respect to the types of VMEDs. It includes information on the year of study, the number of effects, and the research methodologies used, such as numerical analysis and experimentation. This table contains comprehensive information on VMEDs, including the current level of productivity, research trends, and methodology. Because the reviewed studies used different types and amounts of input energy, it is difficult to compare the

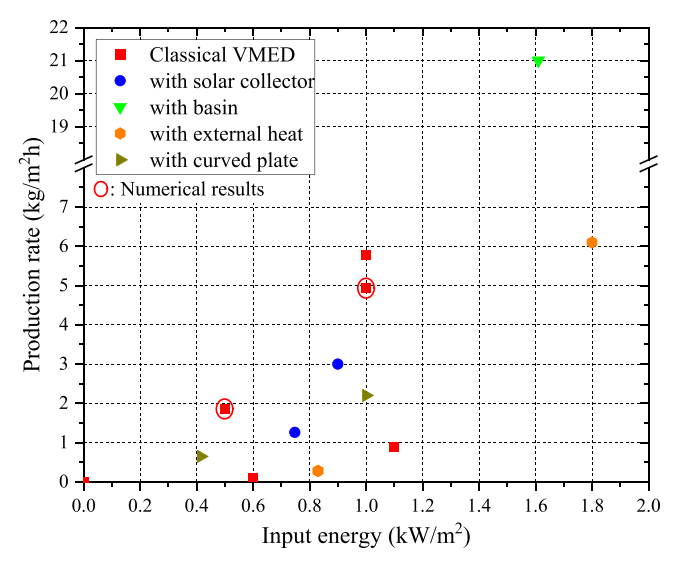
**Table 1**Comparison of productivity according to the type of VMED.

No.	Types	Year	Reference	$N_t$	Heat source	Productivity	Metho
1	Classical VMED	1964	[21]	2	Electric heating pad	$0.898 \text{ kg/(m}^2 \cdot \text{h)} @ 1.1 \text{ kW/m}^2$	Ea
2		1987	[26]	3	Artificial radiation	$1.092 \text{ g/(m}^2 \cdot \text{h)} @ 0.41 \text{ W/m}^2$	E
3		1996	[27]	10	Solar energy	$\cdot 1.85 \text{ kg/(m}^2 \cdot \text{h)} @ 0.5 \text{ kW/m}^2$	$N^a$
						·4.932 kg/(m <sup>2</sup> ·h) @1.0 kW/m <sup>2</sup>	
				1	Electric heater	$0.086 \text{ kg/(m}^2 \cdot \text{h)} @ 0.6 \text{ kW/m}^2$	E
4		1998	[28]	2	Solar energy	$0.84 \text{ kg/(m}^2 \cdot \text{h)} @ T_f = 42.5 ^{\circ}\text{C}$	E
5		2018	[29]	10	Solar energy	$16.6 \text{ kg/(m}^2 \cdot \text{d)} @ Q_{gls} = 23 \text{ MJ/(m}^2 \cdot \text{d)}$	N
6		2020	[31]	3	Solar energy	$\cdot 3.55 \text{ kg/(m}^2 \cdot d) @ Q_{glb} = 10.5 \text{ MJ/(m}^2 \cdot d) \text{ when using WFP}$	E
						$\cdot 3.4 \text{ kg/(m}^2 \cdot d)$ @ $Q_{glb} = 10.5 \text{ MJ/(m}^2 \cdot d)$ when using wick plate	
7		2021	[32]	3	Solar energy	·4.31 kg/(m <sup>2</sup> ·d) @ $Q_{glb} = 9.5 \text{ MJ/(m}^2 \cdot \text{d})$ when using WFP	E
						$\cdot 4.39 \text{ kg/(m}^2 \cdot d)$ @ $Q_{glb} = 9.5 \text{ MJ/(m}^2 \cdot d)$ when using wick plate	
8		2020	[30]	10	Solar energy	$36.0 \text{ kg/(m}^2 \cdot \text{d)} @ Q_{glb} = 25.1 \text{ MJ/(m}^2 \cdot \text{d)}$	N
9		2020	[33]	10	Artificial radiation	$5.78 \text{ kg/(m}^2 \cdot \text{h)} @ 1 \text{ kW/m}^2$	E
					Solar energy	2.6 kg/(kW·h) @ partly sunny day of July	E
10		2020	[34]	3	Solar energy	11.13 kg/(m <sup>2</sup> ·d) (annual average)	N
11	VMED with a solar collector	1961	[35]	6	Electric heater	$14.0 \text{ kg/m}^2 @ T_f = 48.9 ^{\circ}\text{C}$	N
				5		1.26 kg/h	E
12		1987	[37]	2	Solar energy	$2.08 \text{ kg/(m}^2 \cdot \text{d}) @ Q_{gls} = 13.0 \text{ MJ/(m}^2 \cdot \text{d})$	E
				5		6.0 kg/(m <sup>2</sup> ·d) @ April	N
13		2004	[40]	10	Solar energy	21.8 kg/(m <sup>2</sup> ·d) @ $Q_{gls} = 24.4 \text{ MJ/(m}^2 \cdot \text{d}) \text{ and } Q_{glb} = 26 \text{ MJ/}$	N
						(m <sup>2</sup> ·d)	
14		2004	[39]	10	Solar energy	$20.2 \text{ kg/(m}^2 \cdot \text{d)} @ Q_{gls} = 27.4 \text{ MJ/(m}^2 \cdot \text{d)}$	N
15		2005	[38]	4	Artificial radiation	$1.26 \text{ kg/(m}^2 \cdot \text{h)} @ 748 \text{ W/m}^2$	E
16		2014	[41]	10	Solar energy	23.8 kg/(m <sup>2</sup> ·d) with $^{a}$ HR @ $Q_{glb} = 17.3 \text{ MJ/(m}^{2} \cdot \text{d)}$	N
				20	Solar energy	35.8 kg/(m <sup>2</sup> ·d) with HR @ $Q_{glb} = 17.3 \text{ MJ/(m}^2 \cdot \text{d)}$	N
				10	Solar energy	$>3 \text{ kg/(m}^2 \cdot \text{h}) \text{ at } 900 \text{ W/m}^2$	E
17		2016	[42]	5	Solar energy	Annual avg. 21.9 kg/(m <sup>2</sup> ·d)	N
			£3	-	2 2 2 2 2 2 2 2 2 2 2 2 2 2 2 2 2 2 2 2	·Max. 35.57 kg/(m <sup>2</sup> ·d) @ April, 0.25 bar	
18		2020	[43]	5	Solar energy	4.9 kg/(m $^2$ ·d) @ summer (using PCM)	E
19	VMED with an external heat	1984	[44]	3	Electric heat	$4 \text{ kg/(m}^2 \cdot \text{h)} \otimes {}^{\text{a}}\text{T}_{\text{h}} = 90  {}^{\circ}\text{C}$	E
20	source	2001	[45]	4	Hot water	6.1 kg/(m <sup>2</sup> ·h) @ 1.8 kW/m <sup>2</sup> ( $T_h = 96 ^{\circ}\text{C}$ , $T_c = 20 ^{\circ}\text{C}$ )	E
21	source	2005	[46]	19	Hot steam	$13.2 \text{ kg/(m}^2 \cdot \text{h)}$ with 80% $^{\text{a}}\text{HR}$ @ $T_{\text{h}} = 100 ^{\circ}\text{C}$ (steam)	N
22		2011	[48]	2	Waste heat	$0.28 \text{ kg/(m}^2 \cdot \text{h)} @ 0.83 \text{ kW}$	E
23		2011	[47]	1	Waste heat	0.28 kg/(m²·h) @ 0.83 kW	E
24		2011		1	Electric heater	$3.0 \text{ kg/(m}^2 \cdot \text{h)} \oplus 0.33 \text{ kW}$ $3.0 \text{ kg/(m}^2 \cdot \text{h)} \oplus T_h = 85.75 \text{ °C}, T_c = 25.5 \text{ °C (Flat plate)}$	E
24		2016	[49]	1	Electric fleater		E
25		2016	FE13	4	Thomas I on ones, from	$\cdot 7.158 \text{ kg/(m}^2 \cdot \text{h}) @ T_h = 81 \text{ °C}, T_c = 25.5 \text{ °C} (Folded plate)$	E
25		2016	[51]	4	Thermal energy from	$2.935 \text{ kg/(m}^2 \cdot \text{h)} @ {}^{a}T_{h1} = 80-90 \text{ °C}$	E
06	VACED with a self-star	2005	rec1	10	biomass	24.2.1- //2.1) @ Q	
26	VMED with a reflector	2005	[56]	10	Solar energy	$34.2 \text{ kg/(m}^2 \cdot d)$ @ $Q_{glb} = 28 \text{ MJ/(m}^2 \cdot d)$ in spring	N
					0.1	$\cdot 39.7 \text{ kg/(m}^2 \cdot d) @ Q_{glb} = 25.8 \text{ MJ/(m}^2 \cdot d) \text{ in winter}$	
27		2005	[55]	10	Solar energy	$\cdot 29.2 \text{ kg/(m}^2 \cdot \text{d)}$ @ $Q_{glb} = 28 \text{ MJ/(m}^2 \cdot \text{d)}$ in spring	N
				_		$\cdot 34.5 \text{ kg/(m}^2 \cdot d) @ Q_{glb} = 25.8 \text{ MJ/(m}^2 \cdot d) \text{ in winter}$	_
28		2007	[54]	2	Solar energy	4.39 kg/(m <sup>2</sup> ·d) @ $Q_{glb} = 16.8 \text{ MJ/(m}^2 \cdot \text{d)}$	E
29		2007	[53]	10	Solar energy	30–38 kg/(m <sup>2</sup> ·d) throughout the year except winter	N
30	VMED with a basin	2000	[57]	10	Solar energy	15.4 kg/(m <sup>2</sup> ·d) @ $Q_{gls} = 22.4$ MJ/(m <sup>2</sup> ·d) and $Q_{glb} = 26$ MJ/	N
						(m <sup>2</sup> ·d)	
31		2000	[58]	13	Solar energy	22.7 kg/(m <sup>2</sup> ·d) @ $Q_{gls} = 20.2 \text{ MJ/(m}^2 \cdot \text{d})$ and $Q_{glb} = 27.8 \text{ MJ/}$	N
						$(m^2 \cdot d)$	
32		2002	[59]	10	Solar energy	14.8–18.7 kg/(m <sup>2</sup> ·d) @ $Q_{gls} = 20.7–22.4 \text{ MJ/(m}^2 \cdot d)$	E
33		2015	[65]	1	Solar energy	6.015 kg/(m <sup>2</sup> ·d) @ April	N
34		2015	[60]	2	Waste heat	21 kg/(m <sup>2</sup> ·d) @ $Q_{in} = 1.61 \text{ kW/m}^2$	E
35		2016	[61]	10	Waste heat	$18.02 \text{ kg/(m}^2 \cdot \text{d)} @ Q_{in} = 22.37 \text{ MJ/d}$	E
36		2017	[63]	3	Solar energy	$9.89 \text{ kg/(m}^2 \cdot \text{d}) @ Q_{gls} = 24.6 \text{ MJ/(m}^2 \cdot \text{d})$	E
37		2018	[64]	3	Solar energy	9.38 kg/m2 (24 h) @ $Q_{gls} = 23.1 \text{ MJ/(m}^2 \cdot \text{d)}$	E
38		2019	[62]	10	Solar energy	6.63 kg/(m <sup>2</sup> ·d) @ $Q_{glb} = 21.46 \text{ MJ/(m}^2 \cdot \text{d)}$	E
					Waste heat	$6.12 \text{ kg/(m}^2 \cdot \text{d)} @ Q_{in} = 6.4 \text{ MJ}$	E
					Electric heater	$21.65 \text{ kg/(m}^2 \cdot \text{d)}$ @ $Q_{in} = 23.08 \text{ MJ}$	E
39	VMED with a curved-plate	2014	[66]	18	Solar energy	23.9 kg/(m <sup>2</sup> ·d) (based on cover area) @ $Q_{gls} = 22.1 \text{ MJ/(m}^2 \cdot \text{d})$	E
40	•	2015	[67]	3	Solar energy	10.3 kg/(m <sup>2</sup> ·d) @ $Q_{gls} = 26.1 \text{ MJ/(m}^2 \cdot \text{d)}$	N
						$5.74 \text{ kg/(m}^2 \cdot \text{d)} @ Q_{gls} = 22.77 \text{ MJ/(m}^2 \cdot \text{d)}$	E
41		2015	[68]	14	Solar energy	34.7 kg/(m <sup>2</sup> ·d) @ $Q_{gls} = 24.9 \text{ MJ/(m}^2 \cdot d)$	E
42		2020	[69]	6	Solar energy	2.2 kg/(m $^2$ ·h) @ 1 kW/m $^2$ (predicted from laboratory test)	E
		2020	F0>3	Ü		$0.65 \text{ kg/(m}^2 \cdot \text{h})$ @ 415 W/m <sup>2</sup> in outdoor test	-
43	VMED with a tilted wick still	2016	[23]	10	Solar energy	19.2 kg/(m <sup>2</sup> ·d) @ $Q_{glb} = 22.6$ MJ/(m <sup>2</sup> ·d)	N
44	with a thirty wick still	2017	[71]	10	Solar energy	4.88 kg/(m <sup>2</sup> ·d) @ $Q_{glb} = 22.0$ MJ/(m <sup>2</sup> ·d) $Q_{gls} = 18.4$ MJ/	E
7-7		2017	[/ 1]	1	оони спетду	4.00 kg/(iii ·d) (w $Q_{glb} = 13.0$ kg/(iii ·d) $Q_{gls} = 10.4$ kg/(iii ·d) (m <sup>2</sup> ·d)	ь
45		2017	[70]	1	Solar energy	1.36 kg/(m <sup>2</sup> ·d) @ around winter solstice day (for verification)	F
45		2017	[70]	4	Solar energy		E
		2004	[72]	6	Solar energy	39.9 kg/(m <sup>2</sup> ·d) @ $Q_{glb} = 22.6$ MJ/(m <sup>2</sup> ·d) 15 kg/(m <sup>2</sup> ·d) @ $Q_{glb} = 22$ MJ/(m <sup>2</sup> ·d)	N N
				_	0.1		

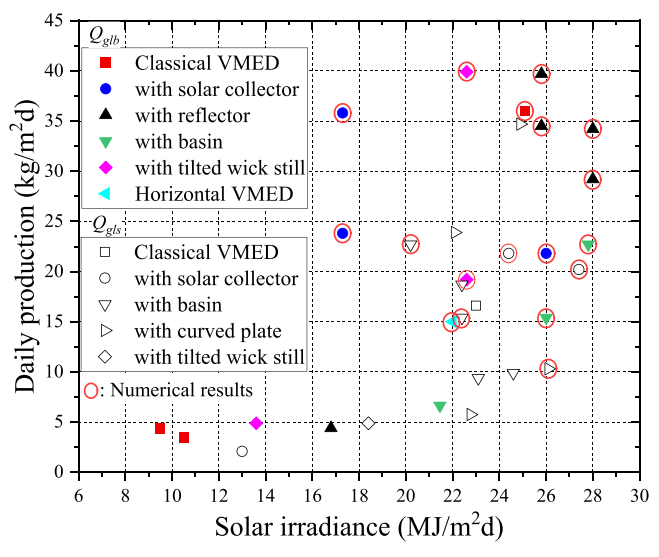
a Note. E: experimental study, N: Numerical study,  $T_h$ : hot-water supply temperature in the first plate,  $T_c$ : cold-water supply temperature in the last plate,  $T_{h1}$ : heated first plate temperature, HR: heat recovery.

production of all VMEDs. This is because  $Q_{in}$  is frequently used when an external heat source such as a heater or collector is employed and  $Q_{glb}$  or  $Q_{gls}$  is used for solar energy.  $Q_{glb}$  and  $Q_{gls}$  denote the total solar radiation incident on the horizontal and inclined surfaces, respectively. Therefore, in this section, freshwater production was analyzed according to three heat sources. When the trend of solar radiation with time was presented only as a graph in the reviewed papers,  $Q_{glb}$  or  $Q_{gls}$  was derived using the graph analysis program, OriginPro.

It is known that the production of the solar distiller commonly increases with the amount of energy input [28]. However, in Fig. 41, such a trend is unclear because different types of VMEDs are compared. Nevertheless, from a macroscopic perspective, there is a tendency for the production to increase with heat input. Fig. 41(a) shows that VMED with a basin produces the most freshwater when using waste heat. When  $Q_{in} = 1.0 \text{ kW/m}^2$ , the classical VMED and VMED with a curved-plate can afford approximately 5.8 and 2.2 kg/( $m^2$ ·h), respectively. VMED with a solar collector and VMED with an external heat source can afford 4.2 and 1.3 kg/( $m^2$ ·h), respectively, when estimating the values from linear extrapolation of data. It can be seen that the production of VMED with a spiral-shaped plate (in the curved-plate type) is remarkably high [Fig. 41 (b)]. Comparing all the results, the production for the VMED with a



(a) Production according to  $Q_{in}$ 



(b) Production according to  $Q_{glb}$  and  $Q_{gls}$ 

Fig. 41. Distillate production with respect to the energy input.

tilted wick still is the highest. Considering that the average production for the CSS is  $\sim$ 5 kg/m² at 20–23 MJ/m² in a day, most models outperformed CSS in the solar environment. The production for the VMED was theoretically  $\sim$ 6.9 times and experimentally  $\sim$ 8 times higher than that of the CSS.

## 6.3. Comparison with experimental and numerical results

In the graph shown in Fig. 41, the red circles denoted the results obtained from numerical analysis. Fig. 41(a) shows that distillate production determined via experimental results was higher than that using numerical results. When  $Q_{in} = 1.0 \text{ kW/m}^2$ , the classical 10-effect VMED obtained 5.7 and 4.93 kg/(m<sup>2</sup>·h) as per the experimental and numerical results, respectively. From linear extrapolation of the three-point results of the VMED, the fresh water production of 9.6 kg/(m<sup>2</sup>·h) can be obtained at  $Q_{in} = 1.61 \text{ kW/m}^2$ . However, at the same  $Q_{in}$  value, VMED with a basin obtained  $\sim\!\!2.2$  times more freshwater. Fig. 41(b) shows that the numerical study seems to overestimate the productivity. The highest production determined from the numerical study is  $\sim$ 40 kg/(m<sup>2</sup>·d) for the VMED with a reflector and a tilted wick still; however, the experimental results showed production of  $<25 \text{ kg/(m}^2 \cdot \text{d})$ . Unfortunately, VMEDs have few experimental results at high-power solar conditions of >20 MJ/(m<sup>2</sup>·d), except for the VMED with a curved-plate and a basin. For the commercialization of the VMED, verification of the production under all operating conditions is essential. In particular, it is imperative to obtain more freshwater on a sunny day to secure the economic feasibility of VMED [30].

The error between the experiment and the numerical results for the VMED production is within 10%, and the errors for each type of VMED are as follows: the classical VMED = 9.1% [30], the VMED with a solar collector = 7% [38], the VMED with an external heat source = 6.5% [44], the VMED with a reflector = 7% [54], the VMED with a basin = 7% [59], the VMED with curved-plate = 9.46% [67], and the VMED with tilted wick still = 9.8% [71]. The main reasons for these errors were the faults that occurred during operation and production, such as feeding rate fluctuation and an uneven diffusion gap.

## 7. Performance parameters of VMED

The performance of the solar distiller is generally affected by three variables: environment, design, and operating parameters. Table 2 shows the effects of each variable on the performance of VMED, which have been summarized from the studies referred in this review. For environmental parameters, solar radiation, ambient temperature, and feedwater temperature positively affected production but wind speed and salinity of feed water affected production negatively. However, the wind for the last plate enhanced condensation due to the cooling effect and thus increased the production [29]. Therefore, installing a double glass cover on the solar absorbing surface and using cooling water or a cooling fan on the last plate helped to increase the production. The effect of the double glass gap and cooling of the last plate will be discussed again in the following design parameter.

For the design parameters, an increase in  $N_t$  results in more distillate output; however, optimum  $N_t$  exists considering the manufacturing cost. As  $N_t$  increases, the production increases but its increasing slope decreases at a specific  $N_t$ . The most expensive part of VMED is an effect plate [30]. Therefore, it is desirable to derive the optimal  $N_t$  through economic analysis such as via payback time or yearly net profit. Based on the payback time, the optimal  $N_t$  of the classical VMED with a double glass cover was 10–15. The narrower the d, the larger the quantity of freshwater obtained; however, a small gap causes lead to contact problems between the effect plates. Decreasing  $\theta$  to a certain extent increases the production for VMED; However, when the values of  $\theta$  and d are too small, contact problem may occur. For reducing d to <5 mm, the number of spacers, the size of the collecting ditch, the droplet size on the condensation surface, and the flatness of the plate needs to be

**Table 2**Effect of VMED parameters on the production.

Parameters		Effect on production	Recommended optimum value
Environmental	Solar radiation	Productivity increases with solar radiation [28,29,34,37,60,62,66–68,71].	N/A
parameters	Room/ambient temperature	·Productivity increases with ambient temperature [34].	N/A
	Wind speed	<ul> <li>Productivity decreases with the wind speed [29].</li> <li>Wind only increases the productivity for the last plate by enhancing the condensation rate of water vapor [34].</li> </ul>	N/A
	Feedwater temperature	Productivity increases with temperature of the feed water [28,29,44,46,50,56,63].	N/A
	Feedwater salinity	Increasing the salinity of feed water decreases the production rate due to an increase in vapor pressure [46,65,67].	N/A
Design parameters	Number of effects, $N_t$	Productivity increases with $N_t$ and then remains constant [23,29,70,30,37,40,41,55,56,58,67].	·7 [67] ·5 for VMED with a solar collector and a PCM [42] ·10–15 for a double-glass cover [30] ·11 for a single glass cover [29]
	Diffusion gap between plates, $d$	•Narrowing the diffusion gap increases the production rate [30,35,39,40,46,50,58,59,70].  If the gap is too narrow, the plate and wick may contact each other and the production water is contaminated.	·9 for <i>d</i> = 3 mm and 11 for <i>d</i> = 5 mm [40] ·5 mm [30,56] ·50 mm [67]
	Inclination on ground, $\theta$	Decreasing the inclination angle increases the production rate [39].  If the still is tilted too much, the flat plate is bent by its weight, making it difficult to maintain the effect gap [29,30].	·40–50° [29,30] ·Near to the latitude values [39]
	Gap in double-glass Cooling of the last plate	Increasing the gap in double-glass increases the production rate [30]. Cooling the last plate increases productivity by enhancing the condensation rate of water vapor [37,44].	·25–30 mm [30] N/A
Operation parameters	Feed flowrate, $\dot{m}_f$	Productivity increases with a decrease in feed flow rate [40,56,58,64,70].  At a given heat input, there is a specific feed flow rate to obtain the maximum yield [29,30,61].  It is advantageous to supply the same flow rate of saline feedwater to all the effects [29,30].	$\dot{m}_f/\dot{m}_e$ : 2 [56], 4.6–2.8 [62] ·7.2 kg/h [67] · $m_{f,1} = 6$ –8 g/min @ $Q_{in} = 6.1$ MJ [61] ·9, 16, 10, and 3 g/min in spring, summer, fall, and winter, respectively [30]
	Operating pressure	Decreasing the operating pressure increases the productivity. [66,67]	N/A

considered. However, Tanaka et al. [59] suggested that even if the gap is reduced, it is possible to maintain a certain distance between the plates using gap spacers. Therefore, the optimal spacing can be further narrowed through future studies. Increasing the gap in double-glass and cooling the last plate of VMED increases the production. However, the double-glass gap also needs to be optimized considering the minimization of weight and size of VMED, and a previous study suggested the gap as 25–30 mm [30].

For operating parameters, an argument for the optimum  $\dot{m}_f$  value differed among studies. One study suggested that the amount of feed water is optimal to supply more than twice the amount of evaporation [56,62]. However, other theoretical and experimental studies [29,30,61] showed that an optimum  $\dot{m}_f$  exists, which depended on the amount of the input energy. Further, these studies showed that it is advantageous to supply the same flow rate of saline feed water to all the effects. Freshwater production increases by reducing the operating pressure using a vacuum pump.

For the commercialization of the VMED, it is necessary to design and manufacture it considering both optimization of the parameters presented above and economic feasibility. Several studies on the parameter optimization have been conducted, however only a few papers have attempted economic analysis on the VMED. For use in remote areas, it is necessary to analyze the economic feasibility of the small capacity desalination system of <100 tons/day. Previous studies found that water cost ranged 10.0–13.3 \$/ton for the classical VMED [30] and 16.0–19.0 \$/ton for VMED with a basin [65]. CSS was in the range of 1.3–6.5 \$/ton [73], multi-effect distillation with solar energy 7.0 \$/ton [73], and RO with solar energy 2.18–15.63 \$/ton [73,74]. From these data, we found that water costs for VMEDs remain high in the harsh commercial market, and that additional studies should be conducted to improve market competitiveness.

## 8. Conclusion and future works

This paper summarizes the design and performance of all the VMEDs studied since 1964. We classified the VMEDs into eight categories: classical type, with a solar collector, with an external heat source, with a reflector, with a basin, with a curved plate, with a tilted wick still, and the horizontal type. By evaluating the research trend on VMEDs, the recently studied models of VMEDs were determined. The production from various types of VMEDs was tabulated and graphed according to the amount of heat input and solar irradiance to analyze the performance. Finally, the findings and conclusions of previous studies regarding all the optimal parameters affecting the VMED performance were summarized. A detailed summary of this review is as follows:

- The classical VMED has been the most studied VMED. Additionally, VMEDs with a basin, a curved plate, and a tilted wick still have been in the spotlight recently.
- · Among various types of VMEDs, the VMED with a basin and a reflector has shown the highest productivity. However, based on experimental results, the VMED with a curved plate has shown the highest PR of 3.5.
- · The optimum number of effects for VMEDs differed among studies because it was determined on the basis of both cost and performance.
- · Although decreasing the gap between the effects increases the productivity of the VMEDs, to date, a minimum value of *d* to stably operate the VMED is 5 mm.
- · For a feed flow rate of operating parameters, it is most realistic to supply an identical flow rate to all the effects because controlling the feed flow rate is difficult considering  $\dot{m}_f/\dot{m}_e$  or solar irradiance in the field

The analyzed results presented in the form of tables and graphs will aid in the development of new VMEDs or the improvement of the performance by comparing the current levels of the technology. In particular, by referring to the optimal or given conditions of the variables, the exact performance comparison of various types of VMEDs enables the commercialization of solar distillers. The following future research themes are recommended on the basis of reviews:

- It is necessary to conduct experimental studies on the classical VMED under various environmental conditions. Similar to CSS, the classical VMED serves as a critical performance indicator for developing and improving other types of VMEDs. Nevertheless, experimental results exist only for specific environmental conditions and have never been obtained under solar conditions that give maximum performance.
- · Previous studies have been focused on the performance of a single unit. Further studies are required on the scaling-up of VMEDs and system optimization to obtain freshwater over hundreds or thousands of kilograms per day.
- · In previous studies, problems such as the wick detachment [31] and the seawater feeding line clogging [42] have been noted. Because the solar still requires a lifetime of more than 10 years, additional studies are needed to ensure the long-term durability of the existing VMEDs.
- · There is a need for research to reduce the manufacturing cost and weight of the product by substituting components such as the metal effect plate and glass cover. Additionally, studies on reliable seawater feeding and freshwater collection units are required, taking into account an on-field operation.
- To increase production by lowering the internal pressure of VMED using a vacuum pump, design technology development and experimental verification are necessary.
- When a constant heat flux as a heat source, such as an electric heater, is used, it is necessary to study the performance characteristics of VMEDs operating in a high energy range of 1 kW/m² or greater energy range. Furthermore, an experimental study under solar conditions exceeding 20 MJ/(m²·d) is required.
- Owing to the side heat loss and the position of the VMED's feedwater inlet, an uneven distribution of temperature and evaporation occurs in the effect plate along with the width direction. As a result, it is necessary to create and validate the VMED 3D numerical analysis model.
- Research is needed to develop an optimized VMED applicable to the field by comparing and analyzing the economic feasibility of VMED models. To compare the total cost, it will be necessary to organize the capital and maintenance costs of each VMED model.

## Declaration of competing interest

All funding sources for this study are listed in the "Acknowledgments" section of the manuscript.

We have no financial interests to declare.

## Acknowledgments

This study was conducted with support from the Korea Institute of Energy Technology Evaluation and Planning (KETEP) and funded by the Ministry of Trade, Industry and Energy, Republic of Korea in 2020 (No. 20203040010240 and 20206900000020).

#### References

- [1] S. Kalogirou, Seawater desalination using renewable energy sources, Prog. Energy Combust. Sci. 31 (2005) 242–281, https://doi.org/10.1016/j.pecs.2005.03.001.
- [2] A.K. Kaviti, A. Yadav, A. Shukla, Inclined solar still designs: a review, Renew. Sust. Energ. Rev. 54 (2016) 429–451, https://doi.org/10.1016/j.rser.2015.10.027.
- [3] K. Sampathkumar, P. Senthilkumar, Utilization of solar water heater in a single basin solar still-an experimental study, Desalination 297 (2012) 8–19, https://doi. org/10.1016/j.desal.2012.04.012.
- [4] H. Panchal, R. Sathyamurthy, Experimental analysis of single-basin solar still with porous fins, Int. J. Ambient Energy 41 (2020), https://doi.org/10.1080/ 01430750.2017.1360206.

- [5] V. Velmurugan, M. Gopalakrishnan, R. Raghu, K. Srithar, Single basin solar still with fin for enhancing productivity, Energy Convers. Manag. 49 (2008) 2602–2608, https://doi.org/10.1016/j.enconman.2008.05.010.
- [6] M.S.S. Abujazar, S. Fatihah, A.E. Kabeel, Seawater desalination using inclined stepped solar still with copper trays in a wet tropical climate, Desalination 423 (2017) 141–148, https://doi.org/10.1016/j.desal.2017.09.020.
- [7] S.A. El-Agouz, Experimental investigation of stepped solar still with continuous water circulation, Energy Convers. Manag. 86 (2014) 186–193, https://doi.org/ 10.1016/j.enconman.2014.05.021.
- [8] P. Singh, P.P. Singh, J. Singh, R.I. Singh, Performance evaluation of micro stepped solar still, Int. Conf. Eng. Manag. (2013) 16–20, https://doi.org/10.13140/ 2.1.4373.5041.
- [9] A.A. El-Sebaii, S.J. Yaghmour, F.S. Al-Hazmi, A.S. Faidah, F.M. Al-Marzouki, A. A. Al-Ghamdi, Active single basin solar still with a sensible storage medium, Desalination 249 (2009) 699–706, https://doi.org/10.1016/j.desal.2009.02.060.
- [10] M. Sakthivel, S. Shanmugasundaram, Effect of energy storage medium (black granite gravel) on the performance of a solar still, Int. J. Energy Res. 32 (2008) 68–82, https://doi.org/10.1002/er.1335.
- [11] B.F. Sharpley, L.M.K. Boelter, Evaporation of water into quiet air: from a one-foot diameter surface, Ind. Eng. Chem. 30 (1938) 1125–1131, https://doi.org/10.1021/ io50346.008
- [12] H. Aburideh, A. Deliou, B. Abbad, F. Alaoui, D. Tassalit, Z. Tigrine, An experimental study of a solar still: application on the sea water desalination of fouka, Procedia Eng. 33 (2012) 475–484, https://doi.org/10.1016/j.proeng.2012.01.1227.
- [13] M. Castillo-Téllez, I. Pilatowsky-Figueroa, Á. Sánchez-Juárez, J.L. Fernández-Zayas, Experimental study on the air velocity effect on the efficiency and fresh water production in a forced convective double slope solar still, Appl. Therm. Eng. 75 (2015) 1192–1200, https://doi.org/10.1016/j.applthermaleng.2014.10.032.
- [14] S. Rashidi, N. Rahbar, M.S. Valipour, J.A. Esfahani, Enhancement of solar still by reticular porous media: experimental investigation with exergy and economic analysis, Appl. Therm. Eng. 130 (2018) 1341–1348, https://doi.org/10.1016/j. applthermaleng.2017.11.089.
- [15] J. Fernández, N. Chargoy, Multi-stage, indirectly heated solar still, Sol. Energy 44 (1990) 215–223, https://doi.org/10.1016/0038-092X(90)90150-B.
- [16] K.S. Reddy, K.R. Kumar, T.S. O'Donovan, T.K. Mallick, Performance analysis of an evacuated multi-stage solar water desalination system, Desalination 288 (2012) 80–92, https://doi.org/10.1016/j.desal.2011.12.016.
- [17] M. Telkes, Solar Still Construction, 1959.
- [18] D. Dsilva, Winfred Rufuss, S. Iniyan, L. Suganthi, P.A. Davies, Solar stills: A comprehensive review of designs, performance and material advances, Renew. Sustain. Energy Rev. 63 (2016) 464–496, https://doi.org/10.1016/j. rser.2016.05.068.
- [19] J.A. Duffie, W.A. Beckman, Solar Engineering of Thermal Processes, John Wiley & Sons. Inc., Hoboken, NJ, USA, 2013, https://doi.org/10.1002/9781118671603.
- [20] C. Elango, N. Gunasekaran, K. Sampathkumar, Thermal models of solar still—a comprehensive review, Renew. Sust. Energ. Rev. 47 (2015) 856–911, https://doi. org/10.1016/j.rser.2015.03.054.
- [21] M. Kudret Selçuk, Design and performance evaluation of a multiple-effect, tilted solar distillation unit, Sol. Energy 8 (1964) 23–30, https://doi.org/10.1016/0038-092X(64)90007-6.
- [22] B.-J. Lim, S.-S. Yu, C.-D. Park, K.-Y. Chung, One-dimensional numerical analysis of the effect of seawater feed rate on multi-effect solar stills, Trans. Korean Soc. Mech. Eng. B 40 (2016) 477–484, https://doi.org/10.3795/KSME-B.2016.40.7.477.
- [23] H. Tanaka, Theoretical analysis of a vertical multiple-effect diffusion solar still coupled with a tilted wick still, Desalination 377 (2016) 65–72, https://doi.org/ 10.1016/j.desal.2015.09.013.
- [24] G. Burgess, K. Lovegrove, in: Solar thermal powered desalination: membrane versus distillation technologies, Cent. Sustain. Energy Syst. Aust. Natl. Univ., Canberra ACT 0200, 2005, pp. 1–8. http://citeseerx.ist.psu.edu/viewdoc/downlo ad?doi=10.1.1.605.1652&rep=rep1&type=pdf.
- [25] P.I. Cooper, The maximum efficiency of single-effect solar stills, Sol. Energy 15 (1973) 205–217, https://doi.org/10.1016/0038-092X(73)90085-6.
- [26] R. Ouahes, C. Ouahes, P. Le Goff, J. Le Goff, A hardy, high-yield solar distiller of brackish water, Desalination 67 (1987) 43–52, https://doi.org/10.1016/0011-9164(87)90230-X.
- [27] K. Ohshiro, T. Nosoko, T. Nagata, A compact solar still utilizing hydrophobic poly (tetrafluoroethylene) nets for separating neighboring wicks, Desalination 105 (1996) 207–217, https://doi.org/10.1016/0011-9164(96)00078-1.
- [28] B. Bouchekima, B. Gros, R. Ouahes, M. Diboun, Performance study of the capillary film solar distiller, Desalination 116 (1998) 185–192, https://doi.org/10.1016/ S0011-9164(98)00194-5
- [29] B.J. Lim, S.S. Yu, K.Y. Chung, C.D. Park, Numerical analysis of the performance of a tiltable multi-effect solar distiller, Desalination 435 (2018) 23–34, https://doi.org/ 10.1016/j.desal.2017.12.035.
- [30] B.-J. Lim, G.-R. Lee, S.-M. Choi, K.-Y. Chung, C.-D. Park, Model optimization and economic analysis of a multi-effect diffusion solar distiller, Desalination 485 (2020), 114446, https://doi.org/10.1016/j.desal.2020.114446.
- [31] G. Lee, T. Ayodha, B. Lim, C. Park, Development of integrated effect plate for performance improvement of multi-effect diffusion solar still, Desalin. Water Treat. 183 (2020) 73–80, https://doi.org/10.5004/dwt.2020.25252.
- [32] G. Lee, S. Cho, B. Lim, S. Choi, C. Park, Experimental study on a novel multi-effect diffusion solar distiller with wick-free plate, Sol. Energy 230 (2021) 250–259, https://doi.org/10.1016/j.solener.2021.10.032.
- [33] Z. Xu, L. Zhang, L. Zhao, B. Li, B. Bhatia, C. Wang, K.L. Wilke, Y. Song, O. Labban, J.H. Lienhard, R. Wang, E.N. Wang, Ultrahigh-efficiency desalination: Via a

- thermally-localized multistage solar still, Energy Environ. Sci. 13 (2020) 830–839, https://doi.org/10.1039/c0ee/d122b
- [34] H. Sharon, K.S. Reddy, S. Gorjian, Parametric investigation and year round performance of a novel passive multi-chamber vertical solar diffusion still: energy, exergy and enviro-economic aspects, Sol. Energy 211 (2020) 831–846, https://doi. org/10.1016/j.solener.2020.10.016.
- [35] R.V. Dunkle, Solar water desalination: the roof type still and a multiple effect diffusion still, in: Int. Dev. Heat Transf, Americal Society of Mechanical Engineer Proceedings, New York, 1961, pp. 895–902.
- [36] P.I. Cooper, J.A. Appleyard, The construction and performance of a three-effect, wick-type, tilted solar still, sun, Work 12 (1967) 4–8.
- [37] T. Kiatsiriroat, S.C. Bhattacharya, P. Wibulswas, Performance analysis of multiple effect vertical still with a flat plate solar collector, Sol. Wind Technol. 4 (1987) 451–457, https://doi.org/10.1016/0741-983X(87)90021-X.
- [38] H. Tanaka, Y. Nakatake, M. Tanaka, Indoor experiments of the vertical multiple-effect diffusion-type solar still coupled with a heat-pipe solar collector, Desalination 177 (2005) 291–302, https://doi.org/10.1016/j.desal.2004.12.012.
- [39] H. Tanaka, Y. Nakatake, K. Watanabe, Parametric study on a vertical multiple-effect diffusion-typesolar still coupled with a heat-pipe solar collector, Desalination 171 (2004) 243–255, https://doi.org/10.1016/j.desal.2004.04.006.
- [40] H. Tanaka, Y. Nakatake, A vertical multiple-effect diffusion-type solar still coupled with a heat-pipe solar collector, Desalination 160 (2004) 195–205, https://doi. org/10.1016/S0011-9164(04)90009-4.
- [41] B.-J. Huang, T.-L. Chong, H.-S. Chang, P.-H. Wu, Y.-C. Kao, Solar distillation system based on multiple-effect diffusion type still, J. Sustain. Dev. Energy, Water Environ. Syst. 2 (2014) 41–50, https://doi.org/10.13044/j.sdewes.2014.02.0004.
- [42] K.S. Reddy, H. Sharon, Active multi-effect vertical solar still: mathematical modeling, performance investigation and enviro-economic analyses, Desalination 395 (2016) 99–120, https://doi.org/10.1016/j.desal.2016.05.027.
- [43] M. Ghadamgahi, H. Ahmadi-Danesh-Ashtiani, S. Delfani, Comparative study on the multistage solar still performance utilizing PCM in variable thicknesses, Int. J. Energy Res. 44 (2020) 4196–4210, https://doi.org/10.1002/er.4941.
- [44] M.M. Elsayed, K. Fathalah, J. Shams, J. Sabbagh, Performance of multiple effect diffusion stills, Desalination 51 (1984) 183–199, https://doi.org/10.1016/0011-016/00095095
- [45] F. Gräter, M. Dürrbeck, J. Rheinländer, Multi-effect still for hybrid solar/fossil desalination of sea- and brackish water, Desalination 138 (2001) 111–119, https://doi.org/10.1016/S0011-9164(01)00252-1.
- [46] T. Nosoko, T. Kinjo, C.D. Park, Theoretical analysis of a multiple-effect diffusion still producing highly concentrated seawater, Desalination 180 (2005) 33–45, https://doi.org/10.1016/j.desal.2004.09.031.
- [47] C.-D. Park, B.-J. Lim, K.-Y. Chung, Experimental results of a seawater distiller utilizing waste heat of a portable electric generator, Desalin. Water Treat. 31 (2011) 134–137. https://doi.org/10.5004/dwt.2011.2367.
- [48] C.-D. Park, B.-J. Lim, K.-Y. Chung, Two-effect distillation of a seawater distiller utilizing waste heat of a small electric generator, Desalin. Water Treat. 33 (2011) 359–364. https://doi.org/10.5004/dwt.2011.2668.
- [49] A.M. Seleem, Development of Vertical Diffusion Solar Still Utilizing Folded Sheets Technology, The American University in Cairo, 2016, https://doi.org/10.1016/ S0011-9164(01)00252-1
- [50] A. Seleem, M. Mortada, M.El Morsi, M. Younan, Parametric study of vertical diffusion still for water desalination, Int. J. Mech. Aerospace, Ind. Mechatronics Eng. 9 (2015) 319–324. http://www.waset.org/publications/10000630.
   [51] H. Tanaka, Thermal distillation system utilizing biomass energy burned in stove by
- [51] H. Tanaka, Thermal distillation system utilizing biomass energy burned in stove by means of heat pipe, Alex. Eng. J. 55 (2016) 2203–2208, https://doi.org/10.1016/j. aei 2016 06 008
- [52] Z.M. Omara, A.E. Kabeel, A.S. Abdullah, A review of solar still performance with reflectors, Renew. Sust. Energ. Rev. 68 (2017) 638–649, https://doi.org/10.1016/ i.rser.2016.10.031.
- [53] H. Tanaka, Y. Nakatake, Numerical analysis of the vertical multiple-effect diffusion solar still coupled with a flat plate reflector: optimum reflector angle and optimum orientation of the still at various seasons and locations, Desalination 207 (2007) 167–178, https://doi.org/10.1016/j.desal.2006.05.020.
- [54] H. Tanaka, Y. Nakatake, Outdoor experiments of a vertical diffusion solar still coupled with a flat plate reflector, Desalination 214 (2007) 70–82, https://doi.org/ 10.1016/j.desal.2006.08.016.

- [55] H. Tanaka, Y. Nakatake, A simple and highly productive solar still: a vertical multiple-effect diffusion-type solar still coupled with a flat-plate mirror, Desalination 173 (2005) 287–300, https://doi.org/10.1016/j.desal.2004.08.035.
- [56] H. Tanaka, Y. Nakatake, Factors influencing the productivity of a multiple-effect diffusion-type solar still coupled with a flat plate reflector, Desalination 186 (2005) 299–310, https://doi.org/10.1016/j.desal.2005.07.005.
- [57] H. Tanaka, T. Nosoko, T. Nagata, A highly productive basin-type-multiple-effect coupled solar still, Desalination 130 (2000) 279–293, https://doi.org/10.1016/ S0011-9164(00)00092-8.
- [58] H. Tanaka, T. Nosoko, T. Nagata, Parametric investigation of a basin-type-multiple-effect coupled solar still, Desalination 130 (2000) 295–304, https://doi.org/10.1016/j.desal.2005.02.046.
- [59] H. Tanaka, T. Nosoko, T. Nagata, Experimental study of basin-type, multiple-effect, diffusion-coupled solar still, Desalination 150 (2002) 131–144, https://doi.org/ 10.1016/S0011-9164(02)00938-4.
- [60] C.D. Park, B.J. Lim, Y.Do Noh, S.S. Lee, K. ul Chung, Parametric performance test of distiller utilizing solar and waste heat, Desalin. Water Treat. 55 (2015) 3303–3309, https://doi.org/10.1080/19443994.2014.946712.
- [61] C.-D. Park, B.-J. Lim, K.-Y. Chung, S.-S. Lee, Y.-M. Kim, Experimental evaluation of hybrid solar still using waste heat, Desalination 379 (2016) 1–9, https://doi.org/ 10.1016/j.desal.2015.10.004.
- [62] S. Yeo, B. Lim, G. Lee, C. Park, Experimental study of effects of different heat sources on the performance of the hybrid multiple-effect diffusion solar still, Sol. Energy 193 (2019) 324–334, https://doi.org/10.1016/j.solener.2019.09.062.
- [63] A.K. Kaushal, M.K. Mittal, D. Gangacharyulu, An experimental study of floating wick basin type vertical multiple effect diffusion solar still with waste heat recovery, Desalination 414 (2017) 35–45, https://doi.org/10.1016/j. desal.2017.03.033.
- [64] G.S. Dhindsa, M.K. Mittal, Experimental study of basin type vertical multiple effect diffusion solar still integrated with mini solar pond to generate nocturnal distillate, Energy Convers. Manag. 165 (2018) 669–680, https://doi.org/10.1016/j. enconman.2018.03.100.
- [65] H. Sharon, K.S. Reddy, Performance investigation and enviro-economic analysis of active vertical solar distillation units, Energy 84 (2015) 794–807, https://doi.org/ 10.1016/j.energy.2015.03.045.
- [66] T.-L. Chong, B.-J. Huang, P.-H. Wu, Y.-C. Kao, Multiple-effect diffusion solar still coupled with a vacuum-tube collector and heat pipe, Desalination 347 (2014) 66–76, https://doi.org/10.1016/j.desal.2014.05.023.
- [67] G. Xie, J. Xiong, H. Liu, B. Xu, H. Zheng, Y. Yang, Experimental and numerical investigation on a novel solar still with vertical ripple surface, Energy Convers. Manag. 98 (2015) 151–160. https://doi.org/10.1016/j.enconman.2015.03.099.
- [68] B.-J. Huang, T.-L. Chong, P.-H. Wu, H.-Y. Dai, Y.-C. Kao, Spiral multiple-effect diffusion solar still coupled with vacuum-tube collector and heat pipe, Desalination 362 (2015) 74–83, https://doi.org/10.1016/j.desal.2015.02.011.
- [69] L. Huang, H. Jiang, Y. Wang, Z. Ouyang, W. Wang, B. Yang, H. Liu, X. Hu, Enhanced water yield of solar desalination by thermal concentrated multistage distiller, Desalination 477 (2020), 114260, https://doi.org/10.1016/j. desal 2019 114260
- [70] H. Tanaka, Parametric investigation of a vertical multiple-effect diffusion solar still coupled with a tilted wick still, Desalination 408 (2017) 119–126, https://doi.org/ 10.1016/j.desal.2017.01.019.
- [71] H. Tanaka, K. Iishi, Experimental study of a vertical single-effect diffusion solar still coupled with a tilted wick still, Desalination 402 (2017) 19–24, https://doi.org/ 10.1016/j.desal.2016.09.031.
- [72] K. Fukui, T. Nosoko, H. Tanaka, T. Nagata, A new maritime lifesaving multiple-effect solar still design, Desalination 160 (2004) 271–283, https://doi.org/10.1016/S0011-9164(04)90029-X.
- [73] A. Al-Karaghouli, L.L. Kazmerski, Energy consumption and water production cost of conventional and renewable-energy-powered desalination processes, Renew. Sust. Energ. Rev. 24 (2013) 343–356, https://doi.org/10.1016/j.rser.2012.12.064.
- [74] M. Thomson, D. Infield, A photovoltaic-powered seawater reverse-osmosis system without batteries, Desalination 153 (2003) 1–8, https://doi.org/10.1016/S0011-9164(03)80004-8